Characterization of pancreatic adenocarcinomas by transcriptome profiling and screening for circulating tumor DNA

Shulin Zhao

Université de Paris

École doctorale ED563

Laboratoire INSERM UMR-S 1138, Eq 26, MEPPOT

Characterization of pancreatic adenocarcinomas by transcriptome profiling and screening for circulating tumor DNA

Caractérisation des adénocarcinomes pancréatiques par le profilage du transcriptome et la recherche d'ADN tumoral circulant

Par Shulin ZHAO

Thèse de doctorat de BIOLOGIE MOLECULAIRE

Dirigée par Pr Jean-Baptiste BACHET

Présentée et soutenue publiquement le 18 Octobre 2021

Devant un jury composé de :

Jean-Baptiste BACHET	PU-PH	Sorbonne Université	Directeur de thèse
Sandrine DABERNAT	PU-PH	Université de Bordeaux	Rapporteure
Juan IOVANNA	DR	Université d'Aix-Marseille	Rapporteur
Jérôme CROS	PU-PH	Université de Paris	Examinateur
Laetitia DAHAN	PU-PH	Université d'Aix-Marseille	Examinatrice
Pierre LAURENT-PUIG	PU-PH	Université de Paris	Examinateur
Magali SVRCEK	PU-PH	Sorbonne Université	Examinatrice
Rémy NICOLLE	CR	Ligue contre le cancer	Examinateur

Université de Paris

LISTE DES ÉLÉMENTS SOUS DROITS

Liste de **tous les éléments retirés** de la version complète de la thèse
faute d'en détenir les droits

Document à intégrer dans la version partielle de la thèse

Illustrations, figures, images...

Légende de l'image	N° de l'image	Page(s) dans la thèse

Articles, chapitres, entretiens cliniques…

Titre du document	N° (si numéroté)	Page(s) dans la thèse
Prognostic Relevance of Pancreatic Adenocarcinoma (PAC) Whole-tumor Transcriptomic Subtypes and Components		46-71
The Presence of Circulating Tumor DNA and Immune Suppressive Tumor Microenvironment Could Explain the Dismal Prognosis of Basal-like Pancreatic Adenocarcinoma		72-83
Preliminary Results of the Metastatic Pancreatic Adenocarcinoma		84-85

Titre :
Caractérisation des adénocarcinomes pancréatiques par le profilage du transcriptome et la recherche d'ADN tumoral circulant

Résumé :
L'adénocarcinome du pancréas (AP) est l'une des tumeurs digestives malignes les plus fréquentes. Malgré le développement du traitement avec une thérapie adjuvante optimisée, l'AP reste le cancer digestif le plus mortel. Caractériser les APs dans les études translationnelles pourrait aider à mieux comprendre l'hétérogénéité des APs, identifier de nouvelles cibles thérapeutiques, et potentiellement aider à mieux définir la stratégie thérapeutique optimale pour chaque patient. Le profilage transcriptomique et la détection de l'ADN tumoral circulant (ADNtc) sont des outils prometteurs. Le but de notre travail était de mieux caractériser les APs en utilisant le séquençage d l'ARN (RNA-seq) et l'ADNtc.
Dans la première étude, nous avons effectué RNA-seq sur une cohorte précédente d'échantillons de APs réséqués qui ont été analysés par la technologie des puces à ARN. Nous avons utilisé la précision et l'analyse complète du transcriptome pour classer les tumeurs avec des scores de composants quantitatifs au lieu de classifications qualitatives de sous-types. A l'aide de nouveaux échantillons inclus, nous avons défini un nouveau modèle pronostique avec les scores des composantes transcriptomiques et les caractéristiques clinicopathologiques (envahissement ganglionnaire et marges de résection). Ce modèle a montré une meilleure performance de pronostic sur la survie sans maladie (DFS) et la survie globale (OS).
La deuxième étude est une étude de cohorte utilisant des échantillons de sang prélevés de manière prospective et consécutive. Les patients avec APs réséquées primaires et sans traitement néoadjuvant ont été recrutés. Nous avons évalué la corrélation entre les signatures transcriptomiques, l'ADNtc et le microenvironnement tumoral chez les patients avec APs réséquées. Notre résultat a montré que les patients dont les tumeurs composées de composants tumoraux dominants de type basal étaient plus susceptibles de présenter des ADNtc et présentaient un état de « désert immunitaire » dans la tumeur.
Nous avons également deux études en cours, incluant des patients atteints de APs métastatiques dans trois essais contrôlés randomisés. Les RNA-seq des prélèvements tumoraux ont été réalisés (n=197). Nous allons étudier le paysage transcriptomique des APs métastatiques, la valeur prédictive de la classification des sous-types à l'efficacité de différents schémas de chimiothérapie et leur corrélation avec la présence d'ADNtc.
Nos études devraient aider à mieux comprendre les sous-types de APs primaires et métastatiques définis sur le transcriptome. Les modèles précis

et complets développés dans nos études pourraient être utiles dans la pratique de la gestion précise des APs.

Mots clefs:
Adénocarcinome du pancréas, séquençage d l'ARN, l'ADN tumoral circulant

Title:
Characterization of pancreatic adenocarcinomas by transcriptome profiling and screening for circulating tumor DNA

Abstract :
Pancreatic adenocarcinoma (PAC) is one of the most common malignant digestive tumors. Despite the development of the treatment with optimized adjuvant therapy, PAC is still the most lethal digestive cancer. Characterize the PAC in translational studies could help to better understand the PACs heterogeneity, identify new therapeutic targets, and potentially help to better define the optimal therapeutic strategy for each patient.
Transcriptomic profiling and the detection of circulating tumor DNA (ctDNA) are promising tools. The aim of our work was to better characterize the PACs using RNA sequencing (RNA-seq) and ctDNA.
In the first study, we have performed RNA-seq on a previous cohort of resected PAC samples that were analyzed by RNA microarray technology. We used the precision and comprehensive analysis of the transcriptome to classify tumors with quantitative component scores instead of qualitative subtype classifications. With the help of new including samples, we defined a new prognosis model with the transcriptomic components scores and clinicopathological characteristics (node invasion and resection margins). This model showed a better prognosis performance on disease-free survival (DFS) and overall survival (OS).
The second study is cohort study using prospectively consecutively collected blood samples. Patients with primary resected PAC and without neoadjuvant therapy were recruited. We evaluated the correlation between transcriptomic signatures, ctDNA, and tumor microenvironment in resected PAC patients. Our result showed that the patients whose tumors composed of dominant basal-like tumor components were more likely to present ctDNA and showed an “immune desert” state in the tumor.
We have also two studies ongoing, including metastatic PAC patients from three randomized controlled trials. The RNA-seq from tumor samples have been performed (n=197). We are going to investigate the transcriptomic landscape of metastatic PACs, the predictive value of subtypes classification to different chemotherapy regimens efficacy, and their correlation with the presence of ctDNA.
Our studies should help the better understanding of primary and metastatic PACs subtypes defined on transcriptome. The precision and comprehensive models develop in our studies could be useful in the practice of precision management of PAC.

Keywords:
Pancreatic adenocarcinoma, RNA sequencing, circulating tumor DNA

Remerciements

À mon Directeur de Thèse

Monsieur le Professeur Jean-Baptiste BACHET

Tu me fais l'honneur de diriger cette Thèse de sciences. Merci de m'avoir donné la chance de formation dans ton équipe. Merci de ton encadrement, ton énergie et ta détermination. Merci aussi pour toutes tes relectures, tes conseils ton soutien lors de la rédaction de la Thèse. Vois dans cette thèse le résultat de ton investissement et la marque de ma profonde reconnaissance.

Aux Rapporteurs de cette Thèse

Madame la Professeure Sandrine DABERNAT

Merci de l'intérêt que vous portez à ce travail en acceptant d'être rapporteure. Vos travaux sur l'oncologie moléculaire vont apporter un regard expert sur ce travail. Veuillez trouver ici l'expression de mon profond respect.

Monsieur le Directeur de Recherche Juan IOVANNA

Merci de l'intérêt que vous portez à ce travail en acceptant d'être rapporteur. Vos travaux sur les mécanismes moléculaires en cancer pancréatique vont apporter un regard expert sur ce travail. Veuillez trouver ici l'expression de mon profond respect.

Aux Mesdames et Monsieur les Membres du Jury

Madame la Professeure Laetitia DAHAN

Merci d'avoir accepté d'évaluer ce travail de thèse. L'étude PRODIGE 35 que vous avez dirigée m'a fourni une importante cohorte pour ce travail. Veuillez trouver ici le témoigne de mon profond respect.

Madame la Professeure Magali SVRCEK

Merci d'avoir accepté de juger ce travail. Merci de ton aide et de tes conseils pendant les préparation et l'interprétation du « tissue micro-array ». Je suis honoré de ta présence dans ce jury.

Monsieur le Professeur Jérôme CROS

Merci d'avoir accepté d'évaluer ce travail de Thèse. Merci de ton aide pour les diagnostics pathologiques. C'était un grand plaisir de travailler avec toi et ton équipe. Je suis honoré de ta présence dans ce jury.

Monsieur le Professeur Pierre LAURENT-PUIG

Vous me faites l'honneur dévaluer ce travail et son intérêt scientifique. Merci de m'avoir fait confiance pour ce travail de Thèse et pour votre accueil au sein du laboratoire. Votre exigence constante a beaucoup apporté à la qualité scientifique de ce travail. C'était un grand plaisir de faire la programmation avec vous. Veuillez trouver ici mes sincères remerciements.

Monsieur le Docteur Rémy NICOLLE

Merci d'avoir accepté de juger ce travail. Je te remercie également de m'avoir formé la base de R et de m'avoir supervisé pour les analyses bio-informatiques et statistiques. Merci également pour les relectures des publications.

Je remercie « Chinese Scholarship Council » pour le financement pendant la formation.

Je remercie toute l'équipe de l'unité INSERM 1138 pour son accueil, sa patience et son aide de tous les jours. Je remercie particulièrement Valérie TALY, Sophie MOUILLET, Delphine Le CORRE, Claire Mulot, Audrey DIDELOT, Virginie POINDESSOUS, Pascale MAZOYER pour leur aide dans laboratoire.

Merci à Daniel PIETRASZ et Olivier CALIEZ, pour les manipulations et les résultats concernant l'ADN tumoral circulant.

Merci pour les plateformes extérieures de l'unité INSERM 1138, Plateforme de Génotypage/Séquençage de l'Institute ICM, Plateforme CIT Program (LNCC), pour leurs soutiens pendant les recherches.

Merci à mon épouse Chenye, ma fille Wendi, mes beaux-parents et mes parents, qui ont plus particulièrement assuré le soutien affectif de ce travail doctoral.

List of the principal abbreviations

ADEX: Aberrantly differentiated endocrine-exocrine

ADM: Acinar-to-ductal metaplasia

AJCC: American Joint Committee on Cancer

CAF: Cancer-associated fibroblast

cfDNA: cell-free DNA

cfRNA: cell-free RNA

CI: Confidence interval

CT: Computerized tomography

ctDNA: Circulating tumor DNA

ddPCR: droplet digital PCR

DFS: Disease-free survival

DNA: Deoxyribonucleic acid

EB: Elution Buffer

EUS: Endoscopic ultrasound

EVs: Extracellular vesicles

exoRNA: exosomes RNA

FFPE: Formalin-fixed paraffin embedded

FNA: Fine needle aspiration

FNB: Fine needle biopsy

FOLFIRINOX: Combination of oxaliplatin, irinotecan, fluorouracil, and leucovorin

GATA 6: GATA binding protein 6

GDP :Guanosine diphosphate

GTP: Guanosine triphosphate

HR: Hazar ratio

ICA: Independent component analysis

ICGC: International Cancer Genome Consortium

ISH: in situ hybridization

miRNA: micro RNA

MMP: Matrix metalloproteinase

MMR: Mismatch repair deficiency

MSI: Microsatellite instability

NMF: Nonnegative matrix factorization

OS: Overall survival

PAC: Pancreatic Adenocarcinoma

PanINs: Pancreatic intraepithelial neoplasms

PARP: Poly(ADP-ribose) polymerase

PB: Purification Beads

PCR: Polymerase chain reaction

PDXs: Patient-derived xenografts

PFS: Progress-free survival

PP: Pancreatic progenitor

PS: Purification Solution

QM-PDA: Quasi-mesenchymal pancreatic ductal adenocarcinoma

RNA-seq: RNA sequencing

RNA: Ribonucleic acid

RTKs: Receptor tyrosine kinases

SMA: Smooth muscle actin

SPAR: SPARC protein

TCGA: The Cancer Genome Atlas

TGF-β: Transforming growth factor-beta

Table of Contents

Part One INTRODUCTION

Pancreatic adenocarcinoma (PAC) is one of the most frequent digestif cancers. According to the GLOBOCAN 2020[1], it accounts for 2.6% of all cancers worldwide. 495,773 patients were diagnosed with PAC in the year of 2020[1]. The gender ratio is close to 1 [1]. The incidence rate increases with age. In all the patients diagnosed in 2020, 396,844 (80%) patients aged over sixty years old. The developed countries (EU and US) showed a higher incidence than other countries[1] (Figure 1). The incidence of new diagnosed PAC is predicted to be nearly doubled in 20 years. The incidence rate will increase even more rapidly in developing and undeveloped countries. (Asia, Latin America and Caribbean, and Africa) (Figure 2). This increase in incidence may be caused by changes in dietary structure and lifestyle changes brought about by changes in industrial structure.

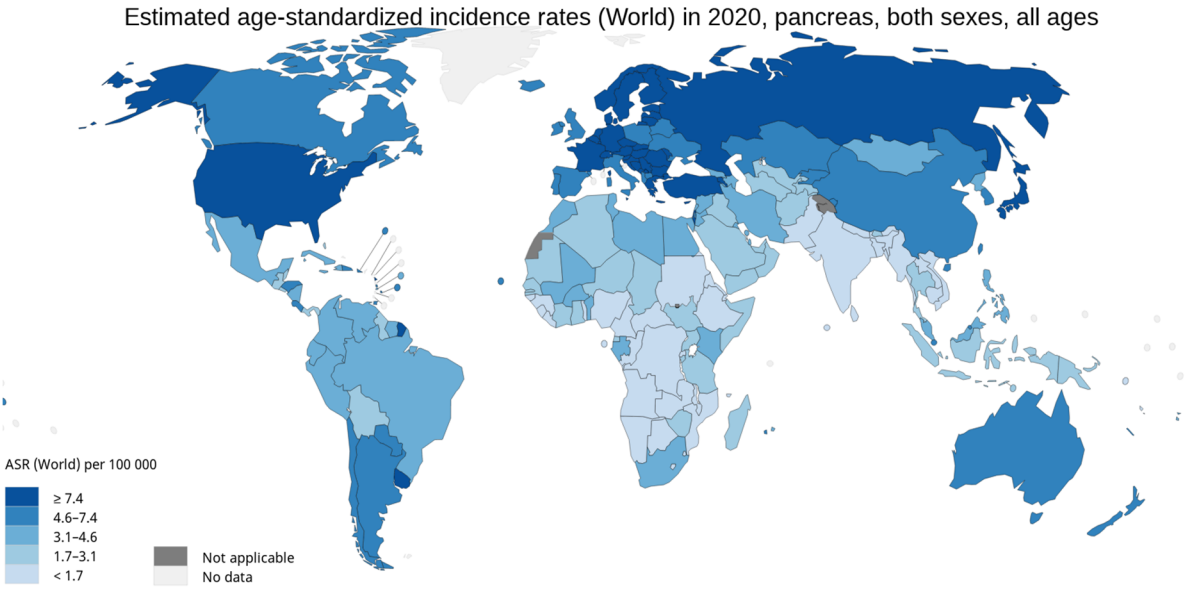

Figure 1. estimated age-standardized incidence rates (World) in 2020, pancreas, both sexes, all ages[1]

PAC is a seriously lethal malignant solid tumor. Despite the relatively low incidence, this cancer is a more lethal and accounts for 4.7% of cancer related mortality. The 5-year overall survival was only 9%, which is the lowest of all cancers[2].

The early detection of PAC is still a challenge for clinical practice. At diagnosis, only 15-20% of patients may benefit from curative resection of their cancer[3]. Systemic chemotherapy is the standard treatment for locally advanced and metastatic PAC.

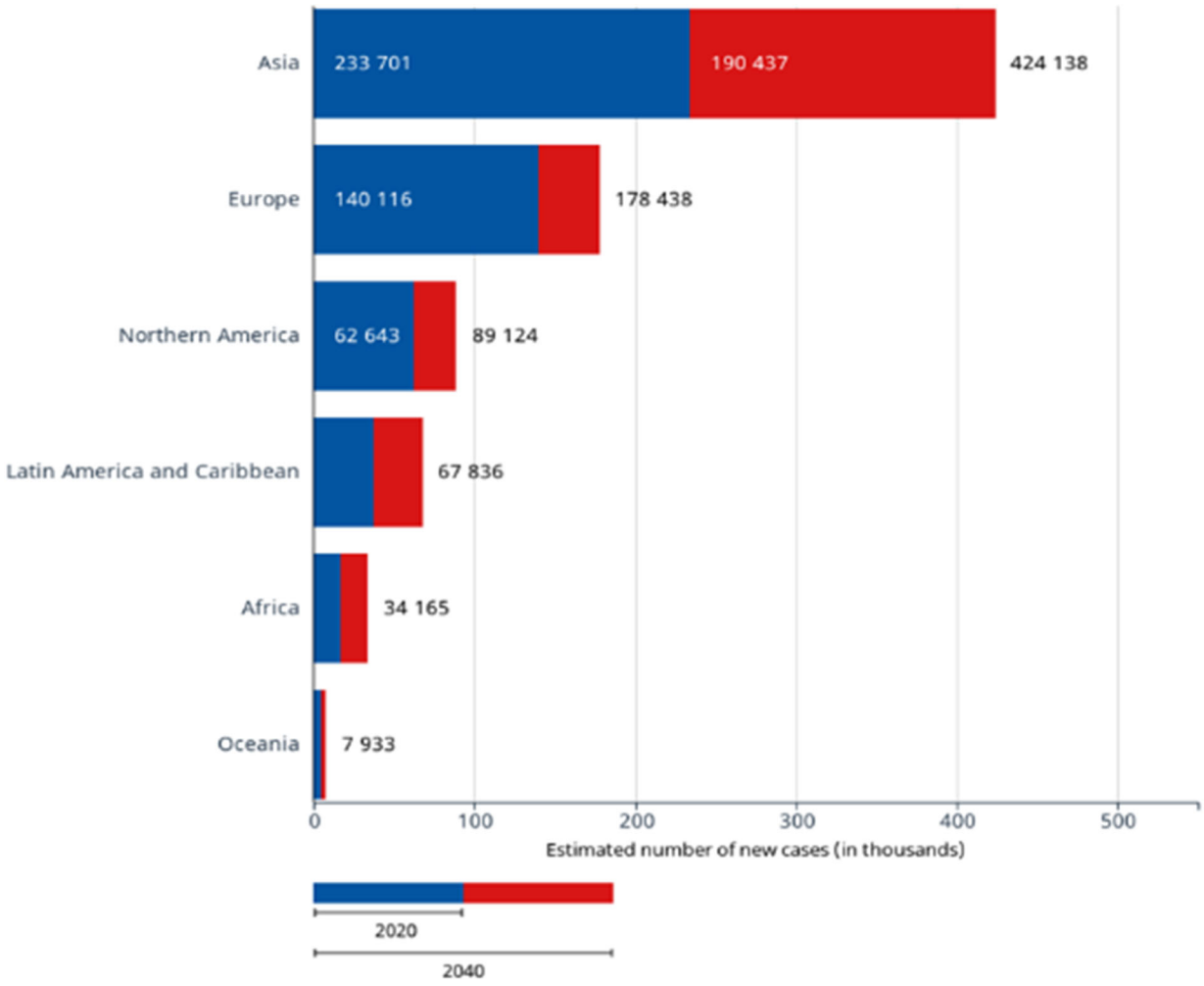

Figure 2. The number of cases of pancreatic cancer in 2020 and the number predicted in 2040[1].

Gemcitabine monotherapy used to be the standard treatment for advanced PAC during over ten years[4]. To improve the prognosis of the advanced PAC, clinical trials of combined regimen were evaluated. In 2011, the result of a phase III clinical trial showed that FOLFIRINOX regimen (combination of oxaliplatin, irinotecan, fluorouracil, and leucovorin) was associated with a survival advantage but with an increased toxicity profile in patients with metastatic PAC[5]. For patients with

resected PAC, using modified FOLFIRINOX regimen as adjuvant therapy also showed significantly longer survival than gemcitabine monotherapy at the expense of a higher incidence of toxic effects[6]. FOLFIRINOX is an option to treat patients with good performance status and normal bilirubinemia level. Another phase III clinical trial showed that the combination of nab-paclitaxel plus gemcitabine significantly improved overall survival, progression-free survival, and response rate in patients with metastatic PAC, but rates of peripheral neuropathy and myelosuppression were increased[7].

Comparing with the progress of chemotherapy, the value of chemoradiotherapy for the PAC treatment is still under discussion. The large clinical trials of chemoradiotherapy did not observe any advantage comparing with chemotherapy only in adjuvant and locally advanced setting[8,9].

To improve the rate of R0 resection and the prognosis of resectable, borderline resectable or locally advanced PAC, scientist are developing neoadjuvant/induction therapeutic strategies combining chemotherapy with or without chemoradiotherapy.[10] The first clinical trial of neoadjuvant therapy for PAC was reported in 2015[11]. However, no statistically significant result was observed in this study. ESPAC-5F study recruited 90 borderline resectable patients and divided them into four arms (immediate surgery, GEMCAP, FOLFIRINOX and CRT). The results showed that there was no difference in resection rate between arms. However, induction therapy had a significant survival benefit compared with immediate surgery[12]. In borderline and locally advanced patients and unresectable patients, several centers reported a high secondary resection rate after induction therapy, which is up to 60%[13,14,15]. FOLFIRINOX was used in these studies and was considered as the most promising regimen.

Despite some recent progresses, there is still a part of PACs remain radio- and chemo resistant and the overall prognosis of patients at all stages has been little improved. To describe the heterogeneity of PACs and the benefit of adjuvant therapy, scientist use molecular biology techniques to better characterize the PACs. Collinson et al[16] reported the world's first transcriptomic profiling of PAC. To predict the benefit of adjuvant gemcitabine, Nicolle et al[17] described a group of Gemcitabine sensitive signatures. These preclinical translational studies showed the necessity to better characterize the PACs using the molecular biology methods and develop the biomarkers to guide the clinical practice.

Part Two: Molecular Characterization of Pancreatic Adenocarcinoma

Chapter 1: Genomic Characters

Characterization of PAC genetic alterations shows the involvement of four major driving genes: *KRAS*, *TP53*, *CDKN2A* and *SMAD4*[18].These genes are involved in the distinct steps of the PAC progression. *KRAS* mutation is the driven event in the formation of PAC[19]. After that, the normal epithelium of pancreatic duct transited to an advancing stage, pancreatic intraepithelial neoplasms (PanINs). When the mutation also happened on the tumor suppressor genes (*TP53*[20], *CDKN2A*[21] or *SMAD4*[22]), the PanINs were sped up and progressed to PAC and metastasized rapidly[23] (Figure 3).

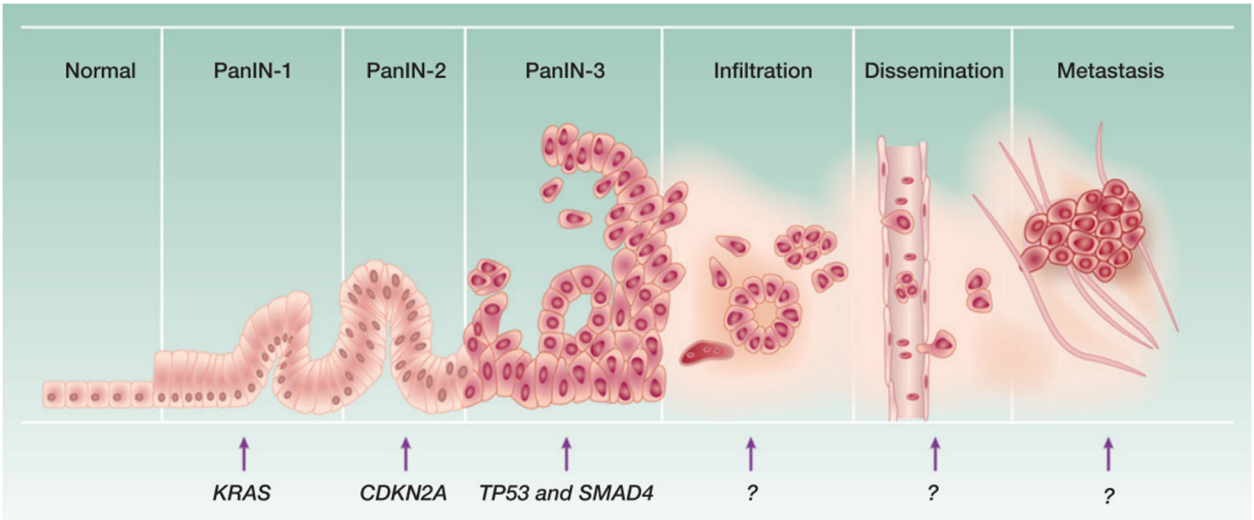

Figure 3. Model of the progression from a normal cell to metastatic pancreatic cancer[19].

KRAS

KRAS mutation was observed in about 90% PAC patients[24]. The mutation of *KRAS* in PAC was usually observed on codon 12, with the most frequent mutations G12D(41%), G12V(34%), and G12R(16%)[23]. The protein *KRAS* is a member of large superfamily of monomeric small (20–25 kDa) GTPases. Diverse cellular processes (cell cycle progression, cell survival, actin cytoskeletal organization, cell polarity and movement, and vesicular and nuclear transport) are regulated by *KRAS*[25]. In normal quiescent cells, *KRAS* is predominantly inactive, with guanosine diphosphate (GDP) bounded. When receptor tyrosine kinases (RTKs) and other cell-surface receptors are activated by extracellular stimuli, *KRAS* is rapid and transient formation active state, with guanosine triphosphate (GTP) bounded. This change leads to control mitogenic processes by regulating a diversity of intracellular signaling networks[26]. Cancer-associated *KRAS* mutations keep *KRAS* persistently and constitutively active state. The effector signaling pathways are over stimulated and drive cancer growth.

There multiple effect pathways are engaged by *KRAS* activation. The most notable pathway is the Raf/Mek/Erk. Through this pathway, *KRAS* plays an important role in activating Hedgehog signaling during PAC tumorigenesis[27]. Another notable pathway is PI3K/Pdk1/Akt. This is a key effector of oncogenic *KRAS* in the pancreas, mediating cell plasticity, acinar-to-ductal metaplasia (ADM), and PAC formation[28]. *KRAS* mutation are also involved in the proliferation of the desmoplastic stroma, who is important in cell proliferation and invasion during PAC development[28].

TP53

TP53 is the coding gene of the p53 protein, whose major function is to maintain genome stability by modulating cellular response to cytotoxic stress. A *TP53* mutation is observed in 50-70% PACs[29]. *TP53* mutation is associated with loss of tumor suppressor pathways. *KRAS* mutation is observed associated with *TP53* alterations[30]. This suggests the effect of tumor genesis of *TP53*[31]. The main mutation of *TP53* is missense mutation, which is often accompanied by loss of the wild-type allele[32]. These results impaired p53 functions occur in late in the progression of PAC[32]. Loss of p53 functions results in aneuploidy and genomic instability, a common observation in PAC[33,34].

SMAD4

SMAD4 is another frequently mutated tumor suppressor gene in PAC. Inactivation of *SMAD4* occurs in 50-60% of the PACs[35]. The *SMAD4* plays an important role in signaling through the transforming growth factor-beta (TGF-β) pathway[36]. TGF-β is proved to be a potent tumor suppressor by inducing anti-proliferation at any phase during cell cycle, especially at the phase G1[37]. Mitogenic signals are blocked by TGF-β through *SMAD4*[38]. TGF-β/*SMAD4* can also induce programmed cell death[39] and apoptosis in PAC[40]. For all the PACs, *SMAD4* homozygous is deleted in 30%, inactivated in 20%, and with an allelic loss of its chromosome in 90%[41]. These genomic mutations of *SMAD4* make the protein degrade more quickly[42]. TGF-β-induced cell cycle arrest and apoptosis are counteracted by the downregulation of *SMAD4*[43]. For PAC patients, loss of *SMAD4* is associated with poor prognosis and widespread metastasis[44]. However, another multi-centric study did not confirm the prognostic value of *SMAD4* , and showed that loss of *SMAD4* may be rather considered as a predictor of benefit from adjuvant chemotherapy[45]. This finding possibly explained the discordant results reported in the literature so far[44].

CDKN2A

CDKN2A is also observed frequently mutated in PAC. The mutation frequency of *CDKN2A* was observed in 49%-98% PACs[46,47]. *CDKN2A* is a tumor suppressor protein and regulates the cell progression by inhibiting cyclinD-CDK4 and cyclinD-CDK6 complexes, thus controlling the progression through the G1/S transition[48]. The mutation of *CDKN2A* is associated with a poor prognostic in PAC patients (HR = 4.52, 95% CI = 1.25–16.35, P = 0.02)[49]. This indicates that *CDKN2A* may be used as a prognostic biomarker in PAC.

Chapter 2: Transcriptomic Characters

Comparing with genomic characteristics, transcriptomic profiling can bring us more abundant characters of PAC. Researchers have started several studies to decipher transcriptomic characters of PAC. Using transcriptomic technology, these studies developed more specific diagnosis and prognosis models and showed promising potential value in the prediction of treatments efficacy.

Collisson's subtyping schema

In 2011, the world first PAC transcriptomic subtyping was published by Collisson et al[16]. In this study, they used microarray technique to profile two merged sets of 27 and 36 primary resected microdissected samples. They performed nonnegative matrix factorization (NMF) analysis with consensus clustering[16] to identify subtypes of PAC. This resulted in a 62 genes signature to define three PAC subtypes: classical, quasi-mesenchymal (QM-PDA) and exocrine-like. The classical subtype had a high expression of adhesion-associated and epithelial genes. The QM-PDA subtype showed high expression of mesenchyme associated genes. The exocrine-like subtype showed relatively high expression of tumor cell derived digestive enzyme genes. The multivariate Cox regression model, including stage and subtypes, suggested subtypes as an independent predictor of overall survival ($p=0.024$). Patients with classical subtypes showed a longer overall survival (OS) than the patients with QM-PDA subtypes after curative intent surgical resection ($p=0.038$). Using PAC cells for validation of this subtyping model, they overlapped the classical and QM-PDA subtypes. However, the exocrine-like subtype was absent, indicating that this subtype might be a contamination of normal pancreas tissue.

They identified two genes associated with this subtyping schema, GATA binding protein 6 (*GATA6*) and v-ki-ras2 kirsten rat sarcoma viral oncogene homolog (*KRAS*). *GATA6*, who is essential for pancreatic development, is highly expressed in most classical subtype tumors and cell lines, and comparatively low in the QM-PDA cell lines and tumors. Classical PDA lines proved to relatively more dependent on *KRAS* than QM-PDA lines. They tested the responses to gemcitabine and erlotinib of the cell lines. QM-PDA subtype lines were, on average, more sensitive to gemcitabine than the classical subtype. Conversely, erlotinib was more effective in classical subtype cell lines.

This pioneer study primarily explored the transcriptomic characteristics of PAC and showed the potential usage to predict the treatments efficacy, as well as to prognosis the survival of the patients.

Kim's subtype schema

Two years after the publication of Collisson, Kim et al[50] identified 3 transcriptomic subtypes of PACs in 2013. Using the RNA microarray technique, the obtained the transcriptomic profiles of

98 PACs. They also used NMF analysis to determine the subtypes. Comparing, with the Collisson's subtype, the subtypes 1 was like the classical subtype. Meanwhile, the immune pathways were also enriched in this subtype. The subtype 2 was similar to QM-PDA subtype and the subtype 3 was similar to exocrine-like subtype. Subtype 2 was more associated with the early metastasis and overall poor prognostic.

Comparing with the mRNA, microRNA (miRNA) regulates the gene expression at the post-transcriptional level[51]. The importance of miRNA in the cancer biology and in the clinical usage has been paid more and more attention in the past two decades[52]. The same Korean team reported three subtypes based on miRNA expression profiles of 104 patients[53]. This 19 miRNAs classifier overlapped the subtypes which they published precedently.

Moffit's subtype schema

Comparing with microarray technique, RNA-seq technique has a broader dynamic range and can detect low abundance transcripts[54]. Moffit et al[55] published the first subtyping schema using both RNA-seq technique and microarray technique. For the training cohort, they used microarray technique to investigate 145 primary and 61 metastatic PACs, 17 cell lines, 46 normal pancreas and 88 distant site adjacent normal samples. Similar to precedent studies, they use NMF to analyze the gene expression. In the validation cohort, they used RNA-seq technique to investigate 15 primary tumors, 37 pancreatic cancer patient-derived xenografts (PDXs), 3 PAC cell lines and 6 cancer-associated fibroblast (CAF) lines derived from unidentified samples collected from patients with PAC.

In this study, they described two tumor subtypes (Classical and basal-like) and two stroma subtypes (normal and activated). The exocrine-like subtype in Collisson's subtype was confirmed as contamination of normal pancreatic exocrine cells. The classical tumor subtype overlapped the classical subtype in Collisson's subtype, and the basal-like tumor subtype was similar to QM-PDA subtype in Collisson's subtype. Normal stroma subtype was characterized by relatively high expression of known markers for pancreatic stellate cells, *ACTA2*, *VIM* and *DES*. The organoid model showed that reducing the motility of pancreatic stellate cells can reduce the proliferation and increase apoptosis of surrounding pancreatic cancer cells[56]. However, the mouse model showed the inverse result[57,58]. Deplete pancreatic stellate cells can enhance the delivery of

chemotherapy[59]. Activated stroma was associated with a more diverse set of genes, such as integrin (ITGAM), chemokine ligands (CCL13 and CCL18), secreting SPARC protein (SPAR), the Wnt family members (WNT2 and WNT5A, MMP9 (gelatinase B) and MMP11 (stromelysin 3). In the multivariate cox-regression, both the tumor type and the stroma type were independent prognostic factors. The basal-like tumor subtype and the activated stroma subtype were associated with poor prognosis. Combining the tumor and the stroma subtype, the patients were divided into four groups. Patients with classic tumor and normal stroma showed the best prognostic (HR 0.39, 95%CI = 0.21-0.73), meanwhile, the patients with basal-like tumor and activated stroma showed the worst prognostic (HR 2.28, 95%CI = 1.34-3.87).

This subtype schema provided new insights into the molecular composition of PAC and could be used for precision medicine. These findings showed the potential usage in the decision support in a clinical setting, where the choice and timing of therapies are critical.

Bailey's subtype schema

In 2016, Bailey et al. and the International Cancer Genome Consortium (ICGC) published the first RNA-seq-based subtype schema[60]. They investigated 96 tumor samples with high epithelial content (≥40%) to balance stromal gene expression. By integrating genomic analysis, they defined four subtypes: squamous, pancreatic progenitor (PP), immunogenic, and aberrantly differentiated endocrine-exocrine (ADEX).

Squamous subtype was similar to Collisson's QM-PDA subtype. These tumors are enriched for *TP53* and *KDM6A* mutations, upregulation of the TP63ΔN transcriptional network, hyper-methylation of pancreatic endodermal cell-fate determining genes and have a poor prognosis. PP subtype was similar to Collisson's classical subtype. These preferentially expressed genes involved in early pancreatic development (*FOXA2/3*, *PDX1* and *MNX1*). ADEX subtype was similar to Collisson's exocrine-like subtype. These tumors displayed upregulation of genes that regulate networks involved in *KRAS* activation, exocrine (*NR5A2* and *RBPJL*), and endocrine differentiation (*NEUROD1* and *NKX2-2*). Immunogenic subtype was a new subtype which was not described previously by other teams. These tumors contained upregulated immune networks, including pathways involved in acquired immune suppression. The novel immunogenic subtype of PAC is characterized by specific mechanisms that might be targeted using immune modulators.

Evaluation and comparison of the published subtype schema by TCGA cohort

The Cancer Genome Atlas (TCGA) consortium validated and compared the published subtype schema by using 150 primary PAC samples[61]. They applied the subtyping method from Collisson et al., Moffit et al., and Bailey et al. They found that classification of samples as basal-like or classical (Moffitt's subtype and Bailey's subtype) was independent of purity. In contrast, the classifications of Collisson's subtype and other subtypes in Bailey's subtype were correlated with tumor purity. Samples classified as exocrine-like or QM-PDA, or ADEX or immunogenic having lower tumor purity. They also found that, among low-purity tumors, a higher estimated leukocyte fraction was associated with immunogenic samples. The ADEX class was a subset of the exocrine-like class. These observations suggested that high-purity tumors could be consistently classified into a basal-like/squamous group and a classical/progenitor group. The strong association of immunogenic and ADEX or exocrine-like subtypes with the low-purity suggested that these subtypes might reflect gene expression from non-neoplastic cells.

Puleo's subtype schema

In 2018, using 309 formalin-fixed paraffin embedded samples, Puleo et al[62] published a new subtype schema. This cohort is the largest cohort comparing with the published cohorts. Transcriptomic profiles were acquired using Affymetrix HG-U219 microarray.

First, they performed an independent component analysis (ICA)[63] on the transcriptomic data set to retrieve the 10 most robust and reproducible independent components. This resulted in each transcriptomic component assigning a weight to each sample. They identified two tumor components (Basal-like and classical) and four stroma components (activated stroma, structural vascular stroma, inflammatory stroma, and immune stroma).

These two tumor components overlapped the tumor subtypes that were previously described[62]. They also confirmed that the exocrine and endocrine components described in the previous subtyping schema were derived from normal pancreatic cell contamination.

- The activated stroma component was defined by high *SPARC*, *FAP*, and *ACTA2* (a-smooth muscle actin [SMA]–coding gene) expression; this stroma component overlapped the active stroma subtype described by Moffitt et al.

- The structural vascularized stroma component was found to be enriched in fibroblast and endothelial cells, expressing elastic fiber and collagen organization genes and low mitotic markers. Enrichment analysis confirmed significant overexpression of activated stroma, extracellular matrix organization, focal adhesion, extracellular matrix receptor interaction, and collagen formation pathway genes.

- The inflammatory stroma component was associated with high expression levels of IL-6 and other markers of inflammation and macrophage activation (NR4A1, NR4A3). Pathway analyzes confirmed enrichment in tumor necrosis factor, interleukin 6, and NFAT signaling pathways.

- The immune stroma component was identified with high expression of immune response genes (CD37, CD53, CD4, CSF1R) and characterized by signatures of multiple actors of immunity (T and B cells, cytotoxic lymphocytes, monocytic lineage, and myeloid dendritic cells). Enrichment analysis showed up-regulation of chemokine signaling, T-cell receptor signaling, and antigen processing and presentation, as well as immune system activation pathway gene overexpression.

With the help of the quantitative transcriptomic components, they defined 5 qualitative whole-tumor transcriptomic subtypes for easier understanding by broad users and application in clinical use. The unsupervised classification of the entire cohort identified 5 molecular subtypes of PAC, which were characterized by their association with transcriptomic components. The subtypes with more basal-like component and classical component were named as pure basal-like subtype and pure classical subtype. The subtype with specially enriched activated component was named as stroma activated. The subtype with particularly a high expression of structural vascularized stroma component was named as desmoplastic. The subtype with enriched classical component and immune component was named as immune classic.

They also evaluated the genomic landscape of the whole tumor transcriptomic subtypes. The *KRAS* mutation Gly12Arg was enriched in classical tumors, whereas Gly12Asp and Gly12Val were prominent mutations in basal-like subtypes.

For the clinical relevance, the pure basal-like subtype had the worst outcome, with a median overall survival (OS) time of 10.3 months, and the pure classical and immune classical subtypes showed

an equivalently good prognosis (median OS values of 43.1 and 37.4 months, respectively). The stroma activated subtype was associated with a bad prognosis (median OS of 20.2 months), although this was better than the OS of the pure basal-like subtype (stroma differences of outcome across subtypes were also observed activated vs pure basal-like log-rank test, P= 0.018). These results were confirmed when analyzing disease-free survival. These results were validated by using the transcriptomic profile of Bailey's subtype schema.

This new classification system allows an integrated stratification of PAC using both the tumor and tumor microenvironment compartments with implications for therapeutic strategies and patient prognosis.

Usage of transcriptomic character in clinical applications

The transcriptomic result of the COMPASS trial showed that the basal-like subtype is chemoresistant and can be distinguished from classical PAC by GATA6 expression[64]. This result was confirmed by RNA in situ hybridization (ISH) by the same team[65]. However, considering the heterogeneity of the tumor, these two tumor components can exist in the same patient. Preclinical models showed that these two components could be modulated by different therapies demonstrating the plasticity of PAC cells that contributes to the heterogeneity of PAC tumors and their intrinsic resistance to a broad spectrum of therapies[66]. Nicolle et al. developed a transcriptomic profile-based model to predict the benefit of adjuvant gemcitabine in PAC patients[17]. These results indicate the potential value of transcriptomic character in the prediction of the adjuvant therapy benefit.

Chapter 3: Characterization with Circulating Tumor DNA

Comparing with tissue-based biomarker, which needs invasive procedure, the plasma-based biomarkers or "liquid biopsy" can also help the diagnosis, prognosis, and prediction in the personalized precision medicine. The primary liquid biopsy biomarkers include circulating tumor

cells (CTCs), circulating tumor DNA (ctDNA) and extracellular vesicles (EVs) and exosomes[67–71].

The detection of ctDNA appears to be a usable tool for the management of patients with PAC. The prognostic value of ctDNA was observed in several studies[72,73,74]. To early predict the efficacy of chemotherapy, to assess minimal residual disease after surgery and recurrence after curative intent resection, ctDNA was considered as a potential useful biomarker[75,76,77]. The detection rate of ctDNA increased from stage I to IV[72], but it is still not detectable in a certain number of patients, even at an advanced stage[78]. The reason for this phenomenon is not clear. There are two major stratergies to detect ctDNA, targeted (such as digital PCR) and non targted (such as NGS). A good correlation betweent these two strategies was observed[74].

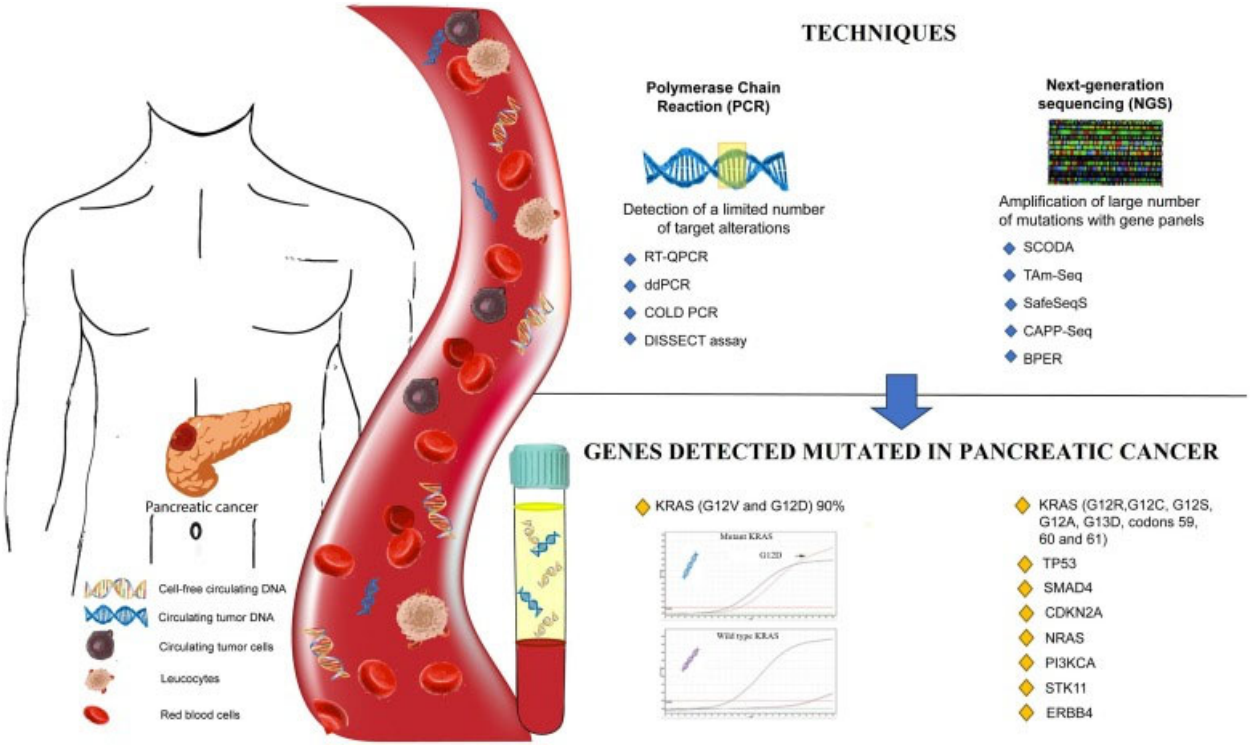

Figure 4. Principles of ctDNA analysis in Pancreatic Adenocarcinoma[74].

Usage of ctDNA in diagnosis

The histology/cytology diagnosis of PAC during the clinical practice is usually based on minimal-invasive procedures, including fine needle aspiration/biopsy (FNA/B) guided by computerized tomography (CT) or endoscopic ultrasound (EUS). A comparative study showed that accuracy of

CT, EUS, and EUS-FNA was 74% (CI 63–83%), 94% (CI 87–98%), and 88% (CI 81–96%), respectively, for diagnosing PAC of all stages pooled[79].

The detection of ctDNA in PAC is usually proceeded by the following techniques: polymerase chain reaction (PCR) test, droplet digital PCR (ddPCR), chip-based digital PCR, methylation-specific PCR, and next-generation sequencing (NGS). The sensitivity of ctDNA detection varies according to PAC stages: from 24.4%~62.2% in resectable patients before surgery[80–83], 48% in locally advanced and metastasis stages[72], 34.6%~64.7% in metastasis stage[84–86]. The large range of sensitivity in each stage might be influenced by the extraction and detection technique[74]. In the studies who included all stages of PAC, ctDNA is more likely to be detected in the later stages[72].

Comparing with image-guided FNA/B, the advantage of diagnostic efficiency was not observed. However, the detection of ctDNA can be proceeded without invasive procedures. Considering this advantage, the detection of ctDNA could be a valuable adjunct to CT for diagnostic evaluation of patients with suspected PAC.

Usage of ctDNA in prognosis

The prognosis value of ctDNA was evaluated in several studies, both in resectable and advanced PAC. In patients with resected PAC, positive ctDNA significantly indicated poor overall survival (pre-operative, HR=2.3, 95% CI: 1.1–4.6; post-operative, HR=3.7, 95% CI 1.5–9.2)[87]. From the same cohort, a trend of higher risk for disease recurrence when ctDNA was detectable (pre-operative, HR=1.96, 95% CI 0.7–5.9; post-operative, HR 2.2, 95% CI 1.0–4.9) [87]. These results were also similarly observed in others independent cohorts[72,88]. For the advanced PAC, the ctDNA detection at the baseline, before chemotherapy beginning, was also described as unfavorable prognostic biomarker[89–92].

According to above studies, the prognosis value of detectable ctDNA in all stages PAC was widely studied. The detectable ctDNA was significantly associated with the dismal prognosis of PAC at all stages.

Usage of ctDNA in the prediction of treatment efficacy

Beyond the applications in the diagnosis and prognosis of PAC, ctDNA can also be used as a biomarker to monitor the response to systemic chemotherapy. In an ancillary study of a phase II clinical trial, ctDNA at baseline and its evolution under treatment had both a prognostic value in patients with metastatic PAC.[74] Moreover, presence of ctDNA could be a predictive biomarker of eryaspase efficacy[75]. Another study indicated that the rate of coincident detection of ctDNA and response to treatment as assessed by CT imaging was 76.9% (10 of 13 cases), and the presence of ctDNA provided the earliest measure of treatment efficacy in 6 of 10 patients (60%)[86].

The genomic profile presented by ctDNA could represent the heterogeneity of PAC more extensively than tumor tissue DNA and allow for monitoring of changes in the molecular makeup during disease progression and under therapy[93]. Currently, some clinical therapeutic application could be used in PAC in accordance with the tissue genomic profiles. For example, PAC presenting mismatch repair deficiency (dMMR; microsatellite instability, MSI) could be eligible for checkpoint inhibitor[94,95]. Patients with PAC and germline *BRCA1/2* mutation benefit from maintenance with PARP inhibitor in case of disease control after a first step of platinum salt based chemotherapy[96]. PAC with *NRG1* gene fusion is targetable by afatinib with promising clinical outcomes[97]. Considering the advantage of the genomic profile from ctDNA over the tumor tissue, the treatments efficacy might be better predicted by ctDNA genomic profile.

Part Three: Patients and Methods

Chapter 1: Patients

RASPANC Cohort

From May 2011 to May 2018, plasmas of all consecutive patients with histologically proven PAC receiving systemic chemotherapy were prospectively collected in the Pitié Salpêtrière Hospital (Paris, France), including resectable and metastatic stages. Blood samples were collected just before (i) the first cycle of adjuvant treatment, after surgical resection in patients who had curative resection (R0/R1), or (ii) the first cycle of chemotherapy in patients with metastatic disease. Blood samples were centrifuged at 3500 rpm for 15 minutes at 4°C within 3 hours of blood draw. Plasma was stored at -80°C until future use. This study was conducted in accordance with principles of the International Conference of Harmonization Good Clinical Practices and Declaration of Helsinki and was approved by an independent ethics committee (CPP Ile-de-France 2014/58NICB and 2014/59NICB). All the patients signed an informed consent form. For metastatic patients, patients without FFPE block available or who had only fine needle aspiration under ultrasound endoscopy were excluded. Pathologist specialized in pancreatic disease (J.A.) confirmed pathology diagnosis, selected representative cores (1 core diameter 1.5 mm for RNA extraction and 4 cores with diameter 1 mm for TMA) after the examination of H&E-stained slide. The following data were collected in a prospective database: clinical and pathologic characteristics (gender, age, medical history, date of diagnosis, location of the primary tumor, primary tumor diameter, tumor differentiation grade, and stage of the disease), follow-up data (date of primary resection, date and type of relapse, date of diagnosis of metastatic disease, date and type of chemotherapy regimen, date and type of chemoradiotherapy, date of death or last follow-up). The TNM stage was redefined according to the AJCC 8th edition by the originally collected data. The R1 resection margin was defined as a distance of the tumor from the resection margin of < or = 1 mm.

Beaujon Cohort

From April 1997 to April 2009, patients with resectable PAC who were operated in Beaujon Hospital (Paris, France) were retrospectively included. Exclusion criteria were preoperative chemotherapy or radiotherapy, macroscopic incomplete resection (R2), ampulla of Vater adenocarcinoma, or pancreatic tumors other than adenocarcinoma. Patients who died of postoperative complications during the 30 days following the surgery were also excluded because they were not informative for translational study. This study was conducted in accordance with principles of the International Conference of Harmonization Good Clinical Practices and Declaration of Helsinki and was approved by an independent ethics committee (CPP Ile-de-France 2014/58NICB and 2014/59NICB). The tumor samples included in this study came from routine care, and no additional samples were taken in the context of this study. An information note was given to the patient to inform them of the use of their samples for future molecular analysis. Patients had the possibility to sign an opposition note for such analysis. All the included patients accepted to participate. Specialist pancreatic pathologist (J.C.) confirmed the presence of neoplastic cells, selected a representative FFPE tumor block after examination of H&E-stained slides and gave a visual estimation of tumor cellularity. Two cores with diameters of 1.5 mm in the zone of tumor were extracted for RNA extraction.

French Multicentric Cohort

This multicentric cohort (Pitié Salpêtrière, Saint Antoine, and Ambroise Paré hospitals) included 165 patients among the 309 patients who were included in our precedent study[62]. For these 165 patients, enough remaining RNA was available. For each case, whole-slide sections were reviewed to select tumor-enriched zones. Two cores with diameters of 1.5 mm were extracted from the paraffin block in this area for RNA/DNA extraction.

PRODIGE 35 Cohort

PRODIGE 35[98] is a prospective, open label, multicenter, randomized phase II trial to evaluate the FOLFIRINOX +/- LV5FU2 maintenance in the first-line treatment of metastatic PAC. There are three arms in this study (NCT02352337): Arm A, FOLFIRINOX every two weeks until the

progression of disease or appearance intolerable toxicity reaction (12 cycles maximum); Arm B, After eight cycles of FOLFIRINOX, in case of disease control, maintenance with LV5FU2 until the progression of disease (resumption of FOLFIRINOX at progression); Arm C, sequential administration of FOLFIRI3 and gemcitabine, alternately every 8 weeks, until progression or unacceptable toxicity. Blood samples were collected at inclusion and sent within 24 hours to the central laboratory. Samples were centrifuged at 3500 rpm for 15 minutes at 4°C. Plasma was stored at -80°C until future use. Specialist pancreatic pathologist (J.C.) confirmed the presence of neoplastic cells, selected a representative FFPE tumor block after examination of H&E-stained slides and gave a visual estimation of tumor cellularity. For the tissue samples, six 10-mm slides were cut and manually microdissected to enrich for neoplastic cells. For the cell aspiration samples, six 10-mm slides were cut, and all the slides were used for RNA/DNA extraction.

PRODIGE 37 Cohort

PRODIGE 37[99] is a prospective, multicenter, randomized phase II trial to evaluate the sequential treatment with nab-paclitaxel + gemcitabine and FOLFIRI3 (alternately) versus Nab-Paclitaxel + Gemcitabine in the first line treatment of metastatic PAC (NCT02827201). There are two arms in this study: Arm A, sequential administration of nab-paclitaxel + gemcitabine and FOLFIRI3, alternately every 8 weeks, until progression or unacceptable toxicity; Arm B, nab-paclitaxel + gemcitabine until progression or unacceptable toxicity. Blood samples were collected at inclusion and sent within 24 hours to the central laboratory. Samples were centrifuged at 3500 rpm for 15 minutes at 4°C. Plasma was stored at -80°C until future use. Specialist pancreatic pathologist (J.C.) confirmed the presence of neoplastic cells, selected a representative FFPE tumor block after examination of H&E-stained slides and gave a visual estimation of tumor cellularity. For the tissue samples, six 10-mm slides were cut and manually microdissected to enrich for neoplastic cells. For the cell aspiration samples, six 10-mm slides were cut, and all the slides were used for RNA/DNA extraction.

AFUGEM Cohort

AFUGEM[100] is a non-comparative, multicenter, open-label, randomized phase II trial to evaluate the nab-paclitaxel plus either gemcitabine or LV5FU2 in the first-line treatment of metastatic PAC

(NCT01964534). There are two arms in this study: Arm A, nab-paclitaxel + gemcitabine until progression or unacceptable toxicity; Arm B, nab-paclitaxel + LV5FU2 until progression or unacceptable toxicity. For the tissue samples, six 10-mm slides were cut and manually microdissected to enrich for neoplastic cells. For the cell aspiration samples, six 10-mm slides were cut, and all the slides were used for RNA extraction.

Chapter 2: Methods

Most of the originally published transcriptomic profiling used RNA extracted from fresh frozen samples. However, fresh frozen samples are not usually available in clinical practice. So, in this study we used formalin fixed paraffin embedded (FFPE) samples. It is complex to extract RNAs from FFPE samples and to analyse transcriptomic profiling using RNA-seq. Because the RNAs are usually degraded in the FFPE samples, it is necessary to use a molecular robust and sensible technique. We will present all the methods used in this thesis in the following text.

Extraction of RNA

The FFPE tumor samples were microdissected from the slices or punched from the FFPE blocks. The zone of tumor was selected and marked by pancreas specialized pathologists under a microscope. The samples were deparaffinized using the deparaffinization solution (Qiagen©, Germany). For the RASPANC cohort, BEAUJON cohort, and AFUGEM cohort, we extracted only the RNAs. The RNeasy FFPE kit (Qiagen©, Germany) was used in the RASPANC cohort and BEAUJON cohort. The miRNeasy FFPE kit (Qiagen©, Germany) was used in the AFUGEM cohort. For the French multicentric cohort, PRODIGE 35 and PRODIGE 37 cohorts, we extracted both DNAs and RNAs at the same time. The ALLPrep FFPE tissue kit (Qiagen©, Venlo, The Netherlands) was used for the double extraction in these cohorts. The extraction was manipulated according to the manufacturer's protocols.

Quantification of extracted RNA by fluorometry

To evaluate the quantity of the RNAs for further study, all the samples were measured after extraction by the fluorometric Qubit® system (Invitrogen, Life Technologies, New York, USA). Considering the high-abundance and broad range of RNA samples, we used the Qubit™ RNA BR Assay Kit as intercalated agent. The assay is highly selective for RNA and will not quantitate DNA, protein, or free nucleotides. Common contaminants, such as salts, free nucleotides, solvents, detergents, or protein, are well tolerated in the assay. The mixed solutions, including agents, samples and two standards, were incubated in the room temperature for about two minutes. The concentrations of samples were displayed directly on the screen of the fluorometer.

RNA sequencing

Since RNA-seq was developed more than a decade ago[101,102], it has become a principal tool to analyze the differential gene expression at transcriptomic level with high-throughput. Actually, the Illumina® platform is the most widely used. After the RNA extraction, the standard workflow includes the following steps: mRNA enrichment, fraction of the whole RNA, cDNA synthesis and preparation of an adaptor-ligated sequencing library, sequencing the library on the high-throughput platform. In this these, we used the RNAs extracted from the FFPE samples. So, the RNAs were already degraded to fragments, and the step of fraction was omitted.

To prepare the library for sequencing, a lot of kits were designed disponible in accordance with different purpose and input materials. In this these, we used two kits who are suitable for RNAs extracted from FFPE samples. We used the Lexogen QuantSeq 3'mRNA-Seq Library Prep Kit FWD (Lexogen Gmbh, Austria) for all the cohorts except the AFUGEM cohort. For the AFUGEM cohort, most of the samples are cytology samples and resulted in a low concentration of RNA solution. The SMARTer Stranded Total RNA-Seq Kit v3 Pico Input Mammalian (Takara Bio, USA) was selected for this cohort because of whose advantage in low concentration input materials.

RNA-seq using the Lexogen QuantSeq 3’mRNA-Seq Library Prep Kit FWD

- **First Strand cDNA Synthesis - Reverse Transcription**

An oligodT primer containing an Illumina-compatible sequence at its 5’ end is hybridized to the RNA and reverse transcription is performed.

1. Mix 150 ng of total RNA in a volume of 5 µl, with 5 µl First Strand cDNA Synthesis Mix 1 in a PCR plate.
2. Prepare a mastermix containing 5 µl First Strand cDNA Synthesis Mix 1, 9.5 µl FS2, and 0.5 µl E1 per sample. Mix well, spin down, and pre-warm for 2 - 3 minutes at 42°C.
3. Add 15 µl of the pre-warmed FS1 / FS2 / E1 mastermix to each 5 µl RNA sample, mix well, and seal the plate. Spin down briefly and incubate the reactions for 1 hour at 42°C.

- **RNA Removal**

During this step, the RNA template was degraded. This is essential for efficient second strand synthesis.

1. Add 10 µl Second Strand Synthesis Mix 1 to the reaction. Mix well by pipetting, seal the plate, and spin down.
2. Incubate for 1 minute at 98°C in a thermocycler and slowly cool down to 25°C at a reduced ramp speed of 0.5°C/second. Incubate the reaction for 30 minutes at 25°C. Quickly spin down the plate before removing the sealing foil.
3. Prepare a mastermix containing 4 µl Second Strand Synthesis Mix 2 and 1 µl Enzyme Mix 2. Mix well.
4. Add 5 µl of the SS2 / E2 mastermix per reaction. Mix well and spin down.
5. Incubate for 15 minutes at 25°C, then briefly spin down.

- **Purification**

The double-stranded library is purified using magnetic beads to remove all reaction components.

1. Add 16 µl of Purification Beads (PB) to each reaction. Mix well and incubate for 5 minutes at room temperature.
2. Place the plate onto a magnet and let the beads collect for 2 - 5 minutes or until the supernatant is completely clear.
3. Remove and discard the clear supernatant without removing the PCR plate from the magnet.
4. Add 40 µl of Elution Buffer (EB), remove the plate from the magnet and resuspend the beads fully in EB. Incubate for 2 minutes at room temperature.
5. Add 48 µl of Purification Solution (PS) to the beads / EB mix to reprecipitate the library. Mix thoroughly and incubate for 5 minutes at room temperature.
6. Place the plate onto a magnet and let the beads collect for 2 - 5 minutes, or until the supernatant is completely clear.
7. Remove and discard the clear supernatant without removing the plate from the magnet.
8. Add 120 µl of 80% EtOH and incubate for 30 seconds. Leave the plate in contact with the magnet as beads should not be resuspended during this washing step. Remove and discard the supernatant.
9. Repeat this washing step once for a total of two washes. Remove the supernatant completely, as traces of ethanol can inhibit subsequent PCR reactions.
10. Leave the plate in contact with the magnet and let the beads dry for 5 - 10 minutes or until all ethanol has evaporated.
11. Add 20 µl of Elution Buffer (EB) per well, remove the plate from the magnet and resuspend the beads fully in EB.
12. Place the plate onto a magnet and let the beads collect for 2 - 5 minutes, or until the supernatant is completely clear.
13. Transfer 17 µl of the clear supernatant into a fresh PCR plate. Do not transfer any beads.

- **QPCR to determine the Optimal Cycle Number for Endpoint PCR**

The mRNA content and quality of total RNA affects the number of PCR cycles needed for the final library amplification step. Variable input types and amounts require optimization of PCR cycle numbers. qPCR assay can optimize the number of cycles required for the endpoint PCR.

1. Dilute the double-stranded library from previous step to 19 µl by adding 2 µl molecular biology-grade water.
2. Prepare a 1:4,000 dilution of SYBR Green I dye in DMSO, for a 2.5x working stock concentration.
3. For each reaction combine: 1.7 µl of the diluted cDNA library, 7 µl of PCR Mix (PCR), 5 µl of P7 Primer (7000), 1 µl of Enzyme Mix (E), and 1.2 µl of 2.5x SYBR Green I nucleic acid dye. Make the total reaction volume up to 30 µl by adding 14.1 µl of molecular biology-grade water.
4. Perform 35 cycles of PCR with the following program: Initial denaturation at 98°C for 30 seconds, 35 cycles of 98°C for 10 seconds, 65°C for 20 seconds and 72°C for 30 seconds, and a final extension at 72°C for 1 minute, hold at 10°C.
5. Using the amplification curves in linear scale, determine the value at which the fluorescence reaches the plateau. Calculate 50% of this maximum fluorescence value and determine at which cycle this value is reached. As the endpoint PCR will contain 10x more cDNA compared to the qPCR, subtract three from this cycle number. This is then the final cycle number you should use for the endpoint PCR with the remaining 17 µl of the template.

- **PCR**

The library is amplified to add the complete adapter sequences required for cluster generation and unique dual indices for multiplexing, and to generate sufficient material for quality control and sequencing.

1. Prepare a mastermix containing 7 µl Dual PCR Mix (Dual PCR) and 1 µl Enzyme Mix (E) per reaction.
2. Add 8 µl of the Dual PCR / E mastermix to 17 µl of the eluted library.
3. Add 10 µl of the respective Unique Dual Index Primer to each sample.
4. Conduct 11 - 25 cycles of PCR (determine the required cycle number by qPCR) with the following program: Initial denaturation at 98°C for 30 seconds, 11 - 25 cycles of 98°C for 10 seconds, 65°C for 20 seconds and 72°C for 30 seconds, and a final extension at 72°C for 1 minute, hold at 10°C.

- **Purification**

The finished library is purified from PCR components that can interfere with quantification.

1. Add 35 µl of thoroughly resuspended Purification Beads (PB) to each reaction.
2. Place the plate onto a magnet and let the beads collect for 2 - 5 minutes or until the supernatant is completely clear.
3. Remove and discard the clear supernatant without removing the PCR plate from the magnet.
4. Add 30 µl of Elution Buffer (EB), remove the plate from the magnet, and resuspend the beads fully in EB. Incubate for 2 minutes at room temperature.
5. Add 30 µl of Purification Solution (PS) to the beads / EB mix to reprecipitate the library. Mix thoroughly and incubate for 5 minutes at room temperature.
6. Place the plate onto a magnet and let the beads collect for 2 - 5 minutes, or until the supernatant is completely clear.
7. Remove and discard the clear supernatant without removing the plate from the magnet. Do not disturb the beads.
8. Add 120 µl of 80% EtOH and incubate the beads for 30 seconds. Leave the plate in contact with the magnet as beads should not be resuspended during this washing step. Remove and discard the supernatant.
9. Repeat this washing step once for a total of two washes. Remove the supernatant completely.
10. Leave the plate in contact with the magnet, and let the beads dry for 5 - 10 minutes or until all ethanol has evaporated.
11. Add 20 µl of Elution Buffer (EB) per well, remove the plate from the magnet, and resuspend the beads fully in EB. Incubate for 2 minutes at room temperature.
12. Place the plate onto a magnet and let the beads collect for 2 - 5 minutes, or until the supernatant is completely clear.
13. Transfer 15 - 17 µl of the supernatant into a fresh PCR plate. Do not transfer any beads. Libraries are now finished and ready for quality control, pooling and cluster generation.

- **RNA sequencing on the platform**

The RNA-seq was performed on the Illumina NovaSeq 6000 platform. A single-read sequencing with 100bp read length and 10 million reads per sample was performed. The fastq document was obtained for each sample after RNA-seq for the further alignment.

RNA-seq using the SMARTer Stranded Total RNA-Seq Kit v3 Pico Input Mammalian

- **First-Strand cDNA Synthesis**

1. Mix the following components on ice: 10 ng of total RNA in a volume of 8 µl, 1 µl SMART Pico Oligos Mix v3.
2. Incubate the tubes at 72°C in a preheated, hot-lid thermal cycler for exactly 3 minutes, then immediately place the samples on an ice-cold PCR chiller rack for 2 minutes.
3. Prepare enough First-Strand Master Mix for all reactions, plus 10%, by combining the following reagents on ice, in the order shown: 4 µl 5X First-Strand Buffer, 4.5 µl SMART TSO Mix v3, 0.5 µl RNase Inhibitor, 2 µl SMARTScribe II Reverse Transcriptase.
4. Add 11 µl of the First-Strand Master Mix to each reaction tube from Step 2. Mix the contents of the tubes by vortexing for 2 sec, then spin the tubes briefly to collect the contents at the bottom.
5. Incubate the tubes in a preheated hot-lid thermal cycler with the following program: 42°C 180 min, 70°C 10 min, 4°C forever.

- **PCR 1**

The indexes (barcodes) that are used to distinguish pooled libraries from each other after sequencing are added at this step.

1. Prepare a PCR 1 Master Mix for all reactions. Combine the following reagents in the order shown, then mix well and spin the tube briefly in a micro-centrifuge: 2 µl Nuclease-free water, 25 µl SeqAmp CB PCR Buffer (2X), 1 µl SeqAmp DNA Polymerase.

2. Add 28 µl of PCR 1 Master Mix to each sample.
3. Add 2 µl of the premixed SMARTer RNA Unique Dual Index primers. Mix by gentle vortexing, then spin down briefly.
4. Place the tubes in a preheated hot-lid thermal cycler. Perform PCR using the following program: 94°C 1 min; 10 cycles: (98°C 15 sec, 55°C 15 sec, 68°C 30 sec), 68°C 2 min, 4°C forever.

- **Purification of RNA-Seq Library Using NucleoMag Beads**

1. Allow NucleoMag beads to come to room temperature before use (~30 min). Add 40 µl of NucleoMag beads to each sample.
2. Incubate at room temperature for 8 minutes to allow the DNA to bind to the beads.
3. Briefly spin the sample tubes to collect the liquid at the bottom. Place the sample tubes on the magnetic separation device for 5 minutes or longer until the solution is completely clear.
4. While the tubes are sitting on the magnetic separation device, pipette out the supernatant and discard.
5. Keeping the tubes on the magnetic separation device, add 200 µl of freshly made 80% ethanol to each sample—without disturbing the beads—to wash away contaminants. Wait for 30 sec and carefully pipette out and discard the supernatant. cDNA will remain bound to the beads during the washing process.
6. Repeat Step 5 once.
7. Remove the tubes from the magnetic separation device. Briefly spin them (~2,000g) to collect the remaining ethanol at the bottom of each tube. Place the tubes back on the magnetic separation device for 30 sec, then—with the tubes still on the device—carefully remove any remaining ethanol with a pipette, without disturbing the beads.
8. Let the open sample tubes rest on the magnetic device at room temperature for 3–5 minutes until the pellets appear dry.

9. Once the beads are dry, add 52 µl of nuclease-free water to cover the beads. Remove the tubes from the magnetic separation device and mix thoroughly by pipetting up and down until all the beads have been washed off the sides of the tubes.
10. Incubate at room temperature for 5 min to rehydrate.
11. Incubate at room temperature for 8 minutes to allow the DNA to bind to the beads. During the incubation time, proceed immediately to next step.

- **Depletion of Ribosomal cDNA with ZapR v3 and R-Probes v3**

In this section, the library fragments originating from rRNA (18S and 28S) and mitochondrial rRNA (m12S and m16S) are cut by ZapR v3 in the presence of R-Probes v3 (mammalian-specific). These R-Probes hybridize to ribosomal RNA and mitochondrial rRNA sequences; however, the mitochondrial sequences are derived from the human mitochondrial genome and are therefore strictly human-specific.

1. Thaw R-Probes v3 and ZapR Buffer at room temperature. Place R-Probes v3 on ice as soon as it is thawed but keep ZapR Buffer at room temperature. ZapR v3 should be kept on ice at all times and returned to the freezer immediately after use.
2. Preheat the thermal cycler in anticipation of Step 5.
3. Upon completion of the 8-min incubation in Step C.14, briefly spin the sample tubes to collect the liquid at the bottom. Place the sample tubes on the magnetic separation device for 5 minutes or longer, until the solution is completely clear.
4. During the 5-min incubation time in the previous step, pipette into a pre-chilled PCR tube a sufficient volume of R-Probes v3 for the number of reactions to be performed (1.5 µl per reaction) plus 10% to account for pipetting errors. Keep the PCR tube containing R-Probes v3 on ice and immediately return the remaining unused R-Probes v3 to a -70°C freezer.
5. Incubate the PCR tube containing R-Probes v3 at 72°C in a preheated hot-lid thermal cycler using the following program: 72°C 2 min, 4°C forever.
6. Leave the R-Probes v3 tube in the thermal cycler at 4°C for at least 2 minutes, but for no more than 10–15 min, before using it.

7. Once the 5-min incubation on the magnetic separation device is complete (Step 3) and the samples are clear, pipette out the supernatant and discard, while keeping the tubes sitting on the magnetic separation device.
8. Keeping the tubes on the magnetic separation device, add 200 µl of freshly made 80% ethanol to each sample—without disturbing the beads—to wash away contaminants. Wait for 30 sec and carefully pipette out and discard the supernatant. cDNA will remain bound to the beads during the washing process.
9. Repeat Step 8 once.
10. Briefly spin the tubes (~2,000g) to collect the remaining ethanol at the bottom of each tube. Place the tubes on the magnetic separation device for 30 sec, then—with the tubes still on the device—carefully remove any remaining ethanol with a pipette, without disturbing the beads.
11. Let the open sample tubes rest at room temperature on the magnetic separation device until the pellets appear dry.
12. While the beads are drying, prepare the ZapR Master Mix. Prepare enough for all reactions, plus 10%, by combining the following reagents at room temperature in the order shown. Add the preheated and chilled R-Probes v3 from Step D.6 last. Return ZapR v3 to a -20°C freezer immediately after use. Mix the components well by vortexing briefly and spin the tubes briefly in a micro-centrifuge. (16.8 µl Nuclease-free water, 2.2 µl 10X ZapR Buffer, 1.5 µl ZapR v3, 1.5 µl R-Probes v3).
13. To each tube of dried NucleoMag beads from Step 11, add 22 µl of the ZapR Master Mix (Step 12). Remove the tubes from the magnetic separation device and mix thoroughly to resuspend the beads.
14. Incubate at room temperature for 5 min to rehydrate.
15. Briefly spin the sample tubes to collect the liquid at the bottom. Place the sample tubes on the magnetic separation device for 1 minutes or longer, until the solution is completely clear.
16. With tubes on the magnetic separation device, pipet out 20 µl of supernatant, being careful not to disturb the beads, into a new PCR strip.

17. Incubate the tubes in a preheated hot-lid thermal cycler using the following program: 37°C 60 min, 72°C 10 min, 4°C forever.

- **PCR 2**

In this section, the library fragments not cleaved by the ZapR v3 reaction in the previous section will be further enriched in a second round of PCR. Since barcodes have already been added to the libraries, a single pair of primers can be used for all libraries.

1. Prepare a PCR 2 Master Mix for all reactions (plus 10%). Combine the following reagents in the order shown, then mix well and spin the tubes briefly in a micro-centrifuge: 26 µl Nuclease-free water, 50 µl SeqAmp CB PCR Buffer, 2 µl PCR2 Primers v3, 2 µl SeqAmp DNA Polymerase.
2. Add 80 µl of PCR 2 Master Mix to each tube from Step D.17. Mix by tapping gently, then spin down.
3. Place the tubes in a preheated hot-lid thermal cycler. Perform PCR using the following program: 94°C 1 min, 10 cycles (98°C 15 sec, 55°C 15 sec, 68°C 30 sec), 4°C forever.

- **Purification of Final RNA-Seq Library Using NucleoMag Beads**

The amplified RNA-seq library is purified by immobilization onto NucleoMag NGS Clean-up and Size Select beads. The beads are then washed with 80% ethanol and eluted in Tris Buffer.

1. Allow NucleoMag beads to come to room temperature before use (~30 min). Add 100 µl of NucleoMag beads to each sample.
2. Incubate at room temperature for 8 minutes to let the cDNA bind to the beads.
3. Briefly spin the sample tubes to collect the liquid at the bottom. Place the sample tubes on the magnetic separation device for 5–10 minutes or longer, until the solution is completely clear.
4. While the tubes are sitting on the magnetic separation device, pipette out the supernatant and discard.
5. Keep the tubes on the magnetic separation device. Without disturbing the beads, add 200 µl of freshly made 80% ethanol to each sample to wash away contaminants. Wait

for 30 sec and carefully pipette out the supernatant. cDNA will remain bound to the beads during the washing process.

6. Repeat Step 5 once.
7. Perform a brief spin of the tubes (~2,000g) to collect the remaining ethanol at the bottom of each tube. Place the tubes on the magnetic separation device for 30 sec, then—with the tubes still on the device—carefully remove all remaining ethanol with a pipette, without disturbing the beads.
8. Let the sample tubes rest open on the magnetic separation device at room temperature for ~5–7 min until the pellets appear dry.
9. Once the beads are dry, add 22 µl of Tris Buffer to cover the beads. Remove the tubes from the magnetic separation device and mix thoroughly by pipetting up and down several times until all the beads have been washed off the sides of the tubes.
10. Incubate at room temperature for 5 min to rehydrate.
11. Briefly spin the sample tubes. Place the sample tubes on the magnetic separation device for 2 minutes or longer, until the solution is completely clear.
12. Transfer 20 µl of supernatants to new tubes.
13. Add 20 µl of NucleoMag beads to perform a second round of beads clean-up by repeating Step 2–8.
14. Once the beads are dry, add 12 µl of Tris Buffer to cover the beads. Remove the tubes from the magnetic separation device and mix thoroughly by pipetting up and down several times until all the beads have been washed off the sides of the tubes.
15. Incubate at room temperature for 5 min to rehydrate.
16. Briefly spin the sample tubes. Place the sample tubes on the magnetic separation device for 2 minutes or longer, until the solution is completely clear.
17. Transfer 10 µl of supernatants to new tubes, and proceed to next step immediately or store in -20°C.

- **RNA sequencing on the platform**

The RNA-seq was performed on the Illumina NovaSeq 6000 platform. A paired-end sequencing with 100bp read length and 2*33 million reads per sample was performed. The fastq document was obtained for each sample after RNA-seq for the further alignment.

Alignment and deriving gene counts matrix

RNAseq reads were mapped using STAR[103] with the proposed ENCODE parameters on the human hg38 genomes and transcript annotation (Ensembl 75). Gene expression profiles were obtained using FeatureCount[104].

Determination of PAC whole-tumor RNA component levels and classification of subtypes previously published

We previously described six RNA components by independent component analysis (ICA)[63] based on Affymetrix result[62,105]. These components can quantitatively describe the composition of the tumor (basal-like tumor component and classical tumor component) and stroma (activated stroma component, inactive structural stroma component, inflammatory stroma component, and immune stroma component). Using the reference of these six components, we projected the component levels of the present study.

We also published[62] the centroid of each of the 5 subtypes (pure classical, immune classical, desmoplastic, stroma activated and pure basal-like). This subtype classification was originally clustered by non-supervised clustering and nominated by their expression of six component levels. The centroid comprises the average subtype expression value of 404 selected genes. The selected gene expression profile of the present study was then correlated to each of the 5 centroids using Spearman rank correlation, as previously published; the subtype centroid with the highest correlation defines the predicted class of the test samples in the present study.

The molecular characterization results in two types of sample phenotyping. Subtyping resulted in a stratification for which each patient is found to be a member of one of the 5 subtypes. On the

other hand, the projection on the 6 components resulted, for each patient, in 6 scores measuring the relative level of each tumor and stromal phenotype encoded by the 6 components. For representation purposes, the component projections were then scaled so that each component had a mean of 0 and standard deviation of 1. Ultimately, the classification into 5 subtypes results in one qualitative variable (with five modalities), while the component projections result in 6 quantitative variables (one for each component).

Construction of TMA and immunohistochemistry

For each FFPE block, four tissue cylinders with diameter 1mm were punched from the center of the tumor. These cylinders were brought into a recipient paraffin block using MTA Booster OI manual tissue arrayer (Alphelys, Plaisir, France). The following primary antibodies were used at the indicated dilutions: anti-CD4 (SP35) rabbit monoclonal primary antibody (dilution 1:4; clone SP35; Ventana, USA); monoclonal mouse anti-human CD8 antibody (dilution 1:100; clone C8/144; Dako, Denmark); monoclonal mouse anti-human CD68 antibody (dilution 1:50; clone KP1; Dako, Denmark); rabbit anti-human FoxP3 monoclonal antibody (dilution 1:100; clone SP97; Spring Bioscience, USA); t-bet monoclonal antibody (dilution 1:100; clone 4B10; eBioscience, USA); PD-1 mouse monoclonal antibody (prediluted; clone NAT105; Sigma-Aldrich, USA); PD-L1 rabbit monoclonal antibody (dilution 1:100; clone NAT105; BIOCYC, Germany). The immunostaining procedure was performed on formalin fixed, deparaffinized, 4 mm thick TMA sections, according to the manufacture's protocol.

Quantification of TMA cores

TMA glass slides were scanned to produce digital slides (0.25 mm/pixel at 40× magnification) using the Aperio Slide Scanning System (ScanScope CS; Aperio Technologies, USA). Positive cells in a square millimeter of CD4, CD8, CD68, FoxP3 and t-bet were counted using software QuPath developed by university of Edinburgh[106]. PD-1 and PD-L1 stained cores were scored by two investigators independently blinded to clinicopathologic information. The percentage of positive cells in the parenchyma of tumors was counted for PD-1. The percentage of positive cells in the parenchyma and mesenchyme of tumors were counted separately for PD-L1. The median value of the 4 scores for every patient was calculated for further statistic study.

Evaluation of Circulating tumor DNA

Blood samples (9 ml) were withdrawn from a central catheter before chemotherapy administration and placed in EDTA tubes. QIAamp Circulating Nucleic Acid Kit (Qiagen, Germany) was used for DNA extraction. Sequencing libraries were prepared from ctDNA using Ion AmpliSeq Colon and Lung Cancer Research Panel v2 (Thermo Fisher, USA). The procedure was performed as described previously[72].

Chapter 3: Object of the work

The team of Professor Pierre Laurent-Puig has focused on the biomarkers of colon cancer and non-small cell lung cancer since several years. With Professor Jean-Baptiste Bachet, the team began some translational studies on PAC. Some interesting finds were reported about ctDNA and transcriptomic profile of PAC by this unit just before my PhD study[72]. I met Professor Bachet during my training as a foreign intern in the Pitié Salpêtrière hospital. And with the help of Chinese scholarship council as well as the kindness of Professor Laurent-Puig and Professor Bachet, a chance to do the PhD study in the team was offered.

The object of this study is to better characterize the PAC using the RNA-seq and ctDNA. We have published/submitted the results obtained in the cohort of patients who had curative intent resection. For the cohorts of metastatic patients, we have finished the manipulations and the statistical analyses are ongoing.

Part Four: Results

The part four has been removed in this partial version of thesis since the copyrights of the articles have been transferred to the journals where the articles are published. (Page 46-85)

La quatrième partie a été retirée de cette version partielle de la thèse puisque les droits d'auteur des articles ont été transférés aux revues où les articles sont publiés. (Page 46-85)

Part Five: Conclusion and Perspectives

Characterization of PACs with RNA-seq and ctDNA is interesting to explore because they can bring us abundant molecular information to better understand the PAC, and the techniques are also clinically applicable. Combining the acquired information could help precision medicine in the future. In this work, firstly, using the profiles acquired by RNA-seq, we validated and compared the qualitative subtypes and quantitative components that were originally developed by our team based on micro-array technique. Both the subtypes and components showed good robustness, while the components were more robust. Another advantage of the components is that could also characterize the PAC more comprehensively. Using the components and clinical-pathological characteristics, we proposed and validated a new prognosis model. Comparing with the subtype-based prognosis model, this model showed a better prognosis performance on disease-free survival (DFS) and overall survival (OS). Secondly, we explored the correlation between the transcriptomic signatures, ctDNA and the tumor immune microenvironment. We found that the patients whose tumors composed of dominant basal-like tumor components were more likely to present ctDNA and showed an "immune desert" status in the tumor.

The results from this study showed that the transcriptomic signatures and ctDNA detection could be used in the clinical management of patients with PAC. However, these results are only initial results, and further studies using the materials from clinical trials are necessary and meaningful. Today, the patients with PAC are clinically staged at diagnosis as resectable, borderline resectable, locally advanced, and metastatic. According to the actual guidelines, all the resectable patients are referred to be operated first. The patients with a borderline resectable or locally advanced PAC receive an induction chemotherapy, follow or not by a chemoradiotherapy, to achieve secondary curative intent surgical resection with R0 margins and improve the prognosis. Systemic chemotherapy is usually proposed to metastatic patients to improve their life quality and overall survival. Under treatment, the prognosis varies largely between patients. Some tumors respond very well under first-line chemotherapy (about one third), half of the tumors are controlled but 10% to 20% are chemo resistant. Today, the 5-FU based (FOLFIRINOX) and Gemcitabine based (nab-

paclitaxel plus gemcitabine) regimens are the two standard first-line protocols. However, we do not have a precise method to predict the treatment response of each patient/tumor. Using the transcriptomic characters could bring us more dimensional information to describe the PAC and might give us a chance to find some molecular signature(s) to predict the treatment response. ctDNA is also another clinically accessible and affordable tool in the management of PAC. Associating transcriptomic profiling and ctDNA information with clinical trials in the future might help us to develop useful molecular signatures and to define an optimal therapeutic strategy for a given patient.

The transcriptomic profiling in this study needs the tissue sample from an invasive procedure. The transcriptomic profiling using "liquid biopsy" samples has not been studied in the patients with PAC. Similar to the cell-free DNA (cfDNA), cell-free RNA or exosomes RNA (exoRNA) could be acquired from the blood samples with non-invasive procedure. Considering that the ctDNA identified from cfDNA can represent the heterogeneity of PAC more extensively than tumor tissue DNA, the same advantage may also exist in the cfRNA/exoRNA profiling. Transcriptomic profiles using blood samples should be studied for the potential benefit in the clinical practice in the future.

With the development of technology advancement, multiomics studies are playing a more and more important role in the oncology research. Comparing with proteome, epigenome, and metabolome, the recently introduced omics technology, genome and transcriptome are more mature and have been well studied. Considering the price quality ratio, genomic and transcriptomic profiles could be more dynamically evaluated during the evolution and the management of PAC. The genomic and transcriptomic based biomarkers are closer to the clinical management. In conclusion, it is necessary to better characterize the PAC using genomic and transcriptomic profiles. Further studies should be designed based on the transitional medicine and precision medicine.

Part Six: Reference

1. Sung H, Ferlay J, Siegel RL, et al. Global Cancer Statistics 2020: GLOBOCAN Estimates of Incidence and Mortality Worldwide for 36 Cancers in 185 Countries. *CA Cancer J Clin*. 2021;71(3):209-249. doi:10.3322/caac.21660
2. Siegel RL, Miller KD, Jemal A. Cancer statistics, 2020. *CA Cancer J Clin*. 2020;70(1):7-30. doi:10.3322/caac.21590
3. Li D, Xie K, Wolff R, Abbruzzese JL. Pancreatic cancer. *Lancet (London, England)*. 2004;363(9414):1049-1057. doi:10.1016/S0140-6736(04)15841-8
4. Howard B, Iii AB, Moore MJ, et al. Improvements in Survival and Clinical Benefit With Gemcitabine as First-Line Therapy for Patients With Advanced Pancreas Cancer : A Randomized Trial. *J Clin Oncol*. 1997;15(6):2403-2413.
5. Conroy T, Desseigne F, Ychou M, et al. FOLFIRINOX versus Gemcitabine for Metastatic Pancreatic Cancer. *N Engl J Med*. 2011;364(19):1817-1825. doi:10.1056/nejmoa1011923
6. Conroy T, Hammel P, Hebbar M, et al. FOLFIRINOX or Gemcitabine as Adjuvant Therapy for Pancreatic Cancer. *N Engl J Med*. 2018;379(25):2395-2406. doi:10.1056/nejmoa1809775
7. Von Hoff DD, Ervin T, Arena FP, et al. Increased Survival in Pancreatic Cancer with nab-Paclitaxel plus Gemcitabine. *N Engl J Med*. 2013;369(18):1691-1703. doi:10.1056/nejmoa1304369
8. Neoptolemos JP, Stocken DD, Friess H, et al. A Randomized Trial of Chemoradiotherapy and Chemotherapy after Resection of Pancreatic Cancer. *N Engl J Med*. 2004;350(12):1200-1210. doi:10.1056/nejmoa032295
9. Hammel P, Huguet F, Van Laethem J-L, et al. Comparison of chemoradiotherapy (CRT) and chemotherapy (CT) in patients with a locally advanced pancreatic cancer (LAPC) controlled after 4 months of gemcitabine with or without erlotinib: Final results of the international phase III LAP 07 study. *J Clin Oncol*. 2013;31(18_suppl):LBA4003-LBA4003. doi:10.1200/jco.2013.31.18_suppl.lba4003
10. Bockhorn M, Uzunoglu FG, Adham M, et al. Borderline resectable pancreatic cancer: A

consensus statement by the International Study Group of Pancreatic Surgery (ISGPS). *Surg (United States)*. 2014;155(6):977-988. doi:10.1016/j.surg.2014.02.001

11. Golcher H, Brunner TB, Witzigmann H, et al. Neoadjuvant chemoradiation therapy with gemcitabine/cisplatin and surgery versus immediate surgery in resectable pancreatic cancer: Results of the first prospective randomized phase II trial. *Strahlentherapie und Onkol*. 2015;191(1):7-16. doi:10.1007/s00066-014-0737-7
12. Ghaneh P, Palmer DH, Cicconi S, et al. ESPAC-5F: Four-arm, prospective, multicenter, international randomized phase II trial of immediate surgery compared with neoadjuvant gemcitabine plus capecitabine (GEMCAP) or FOLFIRINOX or chemoradiotherapy (CRT) in patients with borderline resectable pan. *J Clin Oncol*. 2020;38(15_suppl):4505. doi:10.1200/JCO.2020.38.15_suppl.4505
13. Ferrone CR, Marchegiani G, Hong TS, et al. Radiological and surgical implications of neoadjuvant treatment with FOLFIRINOX for locally advanced and borderline resectable pancreatic cancer. *Ann Surg*. 2015;261(1):12-17. doi:10.1097/SLA.0000000000000867
14. Nitsche U, Wenzel P, Siveke JT, et al. Resectability After First-Line FOLFIRINOX in Initially Unresectable Locally Advanced Pancreatic Cancer: A Single-Center Experience. *Ann Surg Oncol*. 2015;22:1212-1220. doi:10.1245/s10434-015-4851-2
15. Petrelli F, Coinu A, Borgonovo K, et al. FOLFIRINOX-based neoadjuvant therapy in borderline resectable or unresectable pancreatic cancer: A meta-analytical review of published studies. *Pancreas*. 2015;44(4):515-521. doi:10.1097/MPA.0000000000000314
16. Collisson EA, Sadanandam A, Olson P, et al. Subtypes of pancreatic ductal adenocarcinoma and their differing responses to therapy. *Nat Med*. 2011;17(4):500-503. doi:10.1038/nm.2344
17. Nicolle R, Gayet O, Duconseil P, et al. A transcriptomic signature to predict adjuvant gemcitabine sensitivity in pancreatic adenocarcinoma. *Ann Oncol*. 2020;xxx(xxx). doi:10.1016/j.annonc.2020.10.601
18. Notta F, Chan-Seng-Yue M, Lemire M, et al. A renewed model of pancreatic cancer evolution based on genomic rearrangement patterns. *Nature*. 2016;538(7625):378-382. doi:10.1038/nature19823
19. Iacobuzio-Donahue CA, Velculescu VE, Wolfgang CL, Hruban RH. Genetic basis of

pancreas cancer development and progression: Insights from whole-exome and whole-genome sequencing. *Clin Cancer Res*. 2012;18(16):4257-4265. doi:10.1158/1078-0432.CCR-12-0315

20. Hingorani SR, Wang L, Multani AS, et al. Trp53R172H and KrasG12D cooperate to promote chromosomal instability and widely metastatic pancreatic ductal adenocarcinoma in mice. *Cancer Cell*. 2005;7(5):469-483. doi:10.1016/j.ccr.2005.04.023
21. Aguirre AJ, Bardeesy N, Sinha M, et al. Activated Kras and Ink4a/Arf deficiency cooperate to produce metastatic pancreatic ductal adenocarcinoma. *Genes Dev*. 2003;17(24):3112-3126. doi:10.1101/gad.1158703
22. Kojima K, Vickers SM, Adsay NV, et al. Inactivation of Smad4 accelerates KrasG12D-mediated pancreatic neoplasia. *Cancer Res*. 2007;67(17):8121-8130. doi:10.1158/0008-5472.CAN-06-4167
23. Waters AM, Der CJ. KRAS: The critical driver and therapeutic target for pancreatic cancer. *Cold Spring Harb Perspect Med*. 2018;8(9):1-17. doi:10.1101/cshperspect.a031435
24. Jones S, Zhang X, Parsons DW, et al. Core signaling pathways in human pancreatic cancers revealed by global genomic analyses. *Science (80-)*. 2008;321(5897):1801-1806. doi:10.1126/science.1164368
25. Vigil D, Cherfils J, Rossman KL, Der CJ. Ras superfamily GEFs and GAPs: Validated and tractable targets for cancer therapy? *Nat Rev Cancer*. 2010;10(12):842-857. doi:10.1038/nrc2960
26. Sikdar N, Saha G, Dutta A, Ghosh S, Shrikhande S V., Banerjee S. Genetic Alterations of Periampullary and Pancreatic Ductal Adenocarcinoma: An Overview. *Curr Genomics*. 2018;19(6):444-463. doi:10.2174/1389202919666180221160753
27. Koorstra JBM, Hustinx SR, Offerhaus GJA, Maitra A. Pancreatic carcinogenesis. *Pancreatology*. 2008;8(2):110-125. doi:10.1159/000123838
28. Collins MA, Bednar F, Zhang Y, et al. Oncogenic Kras is required for both the initiation and maintenance of pancreatic cancer in mice. *J Clin Invest*. 2012;122(2):639-653. doi:10.1172/JCI59227
29. Eser S, Reiff N, Messer M, et al. Selective requirement of PI3K/PDK1 signaling for kras

oncogene-driven pancreatic cell plasticity and cancer. *Cancer Cell*. 2013;23(3):406-420. doi:10.1016/j.ccr.2013.01.023

30. Kalthoff H, Schmiegel W, Roeder C, et al. p53 and K-RAS alterations in pancreatic epithelial cell lesions. *Oncogene*. 1993;8(2):289-298.

31. Solcia E, Bonato M, Ranzani GN. K-ras and p53 Gene Mutations in Pancreatic Cancer: Ductal and Nonductal Tumors Progress through Different Genetic Lesions. *Cancer Res*. 1994;54(6):1556-1560.

32. Redston MS, Caldas C, Seymour AB, et al. p53 Mutations in Pancreatic Carcinoma and Evidence of Common Involvement of Homocopolymer Tracts in DNA Microdeletions. *Cancer Res*. 1994;54(11):3025-3033. https://cancerres.aacrjournals.org/content/54/11/3025

33. Gorunova L, Höglund M, Andrén-Sandberg Å, et al. Cytogenetic analysis of pancreatic carcinomas: Intratumor heterogeneity and nonrandom pattern of chromosome aberrations. *Genes Chromosom Cancer*. 1998;23(2):81-99. doi:10.1002/(SICI)1098-2264(199810)23:2<81::AID-GCC1>3.0.CO;2-0

34. Harada T, Okita K, Shiraishi K, Kusano N, Kondoh S, Sasaki K. Interglandular cytogenetic heterogeneity detected by comparative genomic hybridization in pancreatic cancer. *Cancer Res*. 2002;62(3):835-839.

35. Hahn SA, Schutte M, Hoque ATMS, et al. able CD21 on B cells without dimlllishing their expression of CD19. 1996;(3):11-14.

36. Sekelsky JJ, Newfeld SJ, Raftery LA, Chartoff EH, Gelbart WM. Genetic characterization and cloning of mothers against dpp, a gene required for decapentaplegic function in Drosophila melanogaster. *Genetics*. 1995;139(3):1347-1358. doi:10.1093/genetics/139.3.1347

37. Massagué J, Blain SW, Lo RS. TGFβ signaling in growth control, cancer, and heritable disorders. *Cell*. 2000;103(2):295-309. doi:10.1016/S0092-8674(00)00121-5

38. Pavlides SC, Lecanda J, Daubriac J, et al. TGF-β activates APC through Cdh1 binding for Cks1 and Skp2 proteasomal destruction stabilizing p27kip1 for normal endometrial growth. *Cell Cycle*. 2016;15(7):931-947. doi:10.1080/15384101.2016.1150393

39. Alvarez C, Bass BL. Role of transforming growth factor-beta in growth and injury

response of the pancreatic duct epithelium in vitro. *J Gastrointest Surg Off J Soc Surg Aliment Tract*. 1999;3(2):178-184. doi:10.1016/s1091-255x(99)80030-4

40. Tachibana I, Imoto M, Adjei PN, et al. Overexpression of the TGFβ-regulated zinc finger encoding gene, TIEG, induces apoptosis in pancreatic epithelial cells. *J Clin Invest*. 1997;99(10):2365-2374. doi:10.1172/JCI119418

41. Sah RP, Saluja A. Molecular mechanisms of pancreatic injury. *Curr Opin Gastroenterol*. 2011;27(5):444-451. doi:10.1097/MOG.0b013e328349e346

42. Xu J, Attisano L. Mutations in the tumor suppressors Smad2 and Smad4 inactivate transforming growth factor β signaling by targeting Smads to the ubiquitin-proteasome pathway. *Proc Natl Acad Sci U S A*. 2000;97(9):4820-4825. doi:10.1073/pnas.97.9.4820

43. Duda DG, Sunamura M, Lefter LP, et al. Restoration of SMAD4 by gene therapy reverses the invasive phenotype in pancreatic adenocarcinoma cells. *Oncogene*. 2003;22(44):6857-6864. doi:10.1038/sj.onc.1206751

44. Goggins M, Shekher M, Turnacioglu K, Yeo CJ, Hruban RH, Kern SE. Genetic alterations of the transforming growth factor β receptor genes in pancreatic and biliary adenocarcinomas. *Cancer Res*. 1998;58(23):5329-5332.

45. Bachet JB, Maréchal R, Demetter P, et al. Contribution of CXCR4 and SMAD4 in predicting disease progression pattern and benefit from adjuvant chemotherapy in resected pancreatic adenocarcinoma. *Ann Oncol*. 2012;23(9):2327-2335. doi:10.1093/annonc/mdr617

46. Chen J, Li D, Killary AM, et al. Polymorphisms of p16, p27, p73, and MDM2 modulate response and survival of pancreatic cancer patients treated with preoperative chemoradiation. *Ann Surg Oncol*. 2009;16(2):431-439. doi:10.1245/s10434-008-0220-8

47. Schutte M, Hruban RH, Geradts J, et al. Abrogation of the Rb/p16 tumor-suppressive pathway in virtually all pancreatic carcinomas. *Cancer Res*. 1997;57(15):3126-3130.

48. Cicenas J, Kvederaviciute K, Meskinyte I, Meskinyte-Kausiliene E, Skeberdyte A. KRAS, TP53, CDKN2A, SMAD4, BRCA1, and BRCA2 mutations in pancreatic cancer. *Cancers (Basel)*. 2017;9(5). doi:10.3390/cancers9050042

49. Tang B, Li Y, Qi G, et al. Clinicopathological Significance of CDKN2A Promoter Hypermethylation Frequency with Pancreatic Cancer. *Sci Rep*. 2015;5(April):1-12.

doi:10.1038/srep13563

50. Kim S, Kang MJ, Lee S, et al. Identifying molecular subtypes related to clinicopathologic factors in pancreatic cancer. *Biomed Eng Online*. 2014;13(Suppl 2):S5. doi:10.1186/1475-925X-13-S2-S5

51. Siomi H, Siomi MC. Posttranscriptional Regulation of MicroRNA Biogenesis in Animals. *Mol Cell*. 2010;38(3):323-332. doi:10.1016/j.molcel.2010.03.013

52. Sun Z, Shi K, Yang S, et al. Effect of exosomal miRNA on cancer biology and clinical applications. *Mol Cancer*. 2018;17(1):1-19. doi:10.1186/s12943-018-0897-7

53. Namkung J, Kwon W, Choi Y, et al. Molecular subtypes of pancreatic cancer based on miRNA expression profiles have independent prognostic value. *J Gastroenterol Hepatol*. 2016;31(6):1160-1167. doi:10.1111/jgh.13253

54. Martens S, Lefesvre P, Nicolle R, et al. Different shades of pancreatic ductal adenocarcinoma, different paths towards precision therapeutic applications. *Ann Oncol*. 2019;30(9):1428-1436. doi:10.1093/annonc/mdz181

55. Moffitt RA, Marayati R, Flate EL, et al. Virtual microdissection identifies distinct tumor- and stroma-specific subtypes of pancreatic ductal adenocarcinoma. *Nat Genet*. 2015;47(10):1168-1178. doi:10.1038/ng.3398

56. Froeling FEM, Feig C, Chelala C, et al. Retinoic acid-induced pancreatic stellate cell quiescence reduces paracrine Wntβ-catenin signaling to slow tumor progression. *Gastroenterology*. 2011;141(4):1486-1497.e14. doi:10.1053/j.gastro.2011.06.047

57. Rhim AD, Oberstein PE, Thomas DH, et al. Stromal elements act to restrain, rather than support, pancreatic ductal adenocarcinoma. *Cancer Cell*. 2014;25(6):735-747. doi:10.1016/j.ccr.2014.04.021

58. Özdemir BC, Pentcheva-Hoang T, Carstens JL, et al. Depletion of carcinoma-associated fibroblasts and fibrosis induces immunosuppression and accelerates pancreas cancer with reduced survival. *Cancer Cell*. 2014;25(6):719-734. doi:10.1016/j.ccr.2014.04.005

59. Olive KP, Jacobetz MA, Davidson CJ, et al. Inhibition of Hedgehog Signaling Enhances Delivery of Chemotherapy in a Mouse Model of Pancreatic Cancer. *Cancer Res*. 2010;324(5933):1457-1461. doi:10.1126/science.1171362.Inhibition

60. Bailey P, Chang DK, Nones K, et al. Genomic analyses identify molecular subtypes of

pancreatic cancer. *Nature*. 2016;531(7592):47-52. doi:10.1038/nature16965

61. Raphael BJ, Hruban RH, Aguirre AJ, et al. Integrated Genomic Characterization of Pancreatic Ductal Adenocarcinoma. *Cancer Cell*. 2017;32(2):185-203.e13. doi:10.1016/j.ccell.2017.07.007

62. Puleo F, Nicolle R, Blum Y, et al. Stratification of Pancreatic Ductal Adenocarcinomas Based on Tumor and Microenvironment Features. *Gastroenterology*. 2018;155(6):1999-2013.e3. doi:10.1053/j.gastro.2018.08.033

63. Cardoso JF, Souloumiac A. Blind beamforming for non-Gaussian signals. *IEE Proceedings, Part F Radar Signal Process*. 1993;140(6):362-370. doi:10.1049/ip-f-2.1993.0054

64. Aung KL, Fischer SE, Denroche RE, et al. HHS Public Access Cancer : Early Results from the COMPASS Trial. *Clin Cancer Res*. 2019;24(6):1344-1354. doi:10.1158/1078-0432.CCR-17-2994.Genomics-Driven

65. O'Kane GM, Grunwald BT, Jang GH, et al. GATA6 Expression Distinguishes Classical and Basal-like Subtypes in Advanced Pancreatic Cancer. *Clin Cancer Res*. 2020;26(18):4901-4910. doi:10.1158/1078-0432.CCR-19-3724

66. Porter RL, Magnus NKC, Thapar V, et al. Epithelial to mesenchymal plasticity and differential response to therapies in pancreatic ductal adenocarcinoma. *Proc Natl Acad Sci U S A*. 2019;116(52):26835-26845. doi:10.1073/pnas.1914915116

67. Vaidyanathan R, Soon RH, Zhang P, Jiang K, Lim CT. Cancer diagnosis: from tumor to liquid biopsy and beyond. *Lab Chip*. 2019;19(1):11-34. doi:10.1039/c8lc00684a

68. Ignatiadis M, Sledge GW, Jeffrey SS. Liquid biopsy enters the clinic - implementation issues and future challenges. *Nat Rev Clin Oncol*. 2021;18(5):297-312. doi:10.1038/s41571-020-00457-x

69. Von Felden J, Garcia-Lezana T, Schulze K, Losic B, Villanueva A. Liquid biopsy in the clinical management of hepatocellular carcinoma. *Gut*. 2020;69(11):2025-2034. doi:10.1136/gutjnl-2019-320282

70. Hofman P, Heeke S, Alix-Panabières C, Pantel K. Liquid biopsy in the era of immuno-oncology: Is it ready for prime-time use for cancer patients? *Ann Oncol*. 2019;30(9):1448-1459. doi:10.1093/annonc/mdz196

71. Normanno N, Cervantes A, Ciardiello F, De Luca A, Pinto C. The liquid biopsy in the management of colorectal cancer patients: Current applications and future scenarios. *Cancer Treat Rev*. 2018;70:1-8. doi:10.1016/j.ctrv.2018.07.007

72. Pietrasz D, Pécuchet N, Garlan F, et al. Plasma circulating tumor DNA in pancreatic cancer patients is a prognostic marker. *Clin Cancer Res*. 2017;23(1):116-123. doi:10.1158/1078-0432.CCR-16-0806

73. Kaczor-Urbanowicz KE, Cheng J, King JC, et al. Reviews on Current Liquid Biopsy for Detection and Management of Pancreatic Cancers. *Pancreas*. 2020;49(9):1141-1152. doi:10.1097/MPA.0000000000001662

74. Abdallah R, Taly V, Zhao S, et al. Plasma circulating tumor DNA in pancreatic adenocarcinoma for screening, diagnosis, prognosis, treatment and follow-up: A systematic review. *Cancer Treat Rev*. 2020;87:102028. doi:10.1016/j.ctrv.2020.102028

75. Bachet JB, Blons H, Hammel P, et al. Circulating Tumor DNA is Prognostic and Potentially Predictive of Eryaspase Efficacy in Second-line in Patients with Advanced Pancreatic Adenocarcinoma. *Clin Cancer Res*. 2020;26(19):5208-5216. doi:10.1158/1078-0432.CCR-20-0950

76. Jiang J, Ye S, Xu Y, et al. Circulating Tumor DNA as a Potential Marker to Detect Minimal Residual Disease and Predict Recurrence in Pancreatic Cancer. *Front Oncol*. 2020;10(July):1-8. doi:10.3389/fonc.2020.01220

77. Yin L, Pu N, Thompson ED, Miao Y, Wolfgang CL, Yu J. Improved assessment of response status in patients with pancreatic cancer treated with neoadjuvant therapy using somatic mutations and liquid biopsy analysis. *Clin Cancer Res*. Published online 2020:clincanres.1746.2020. doi:10.1158/1078-0432.ccr-20-1746

78. Manuscript A, Malignancies H. Detection of Circulating Tumor DNA in Early- and Late-Stage Human Malignancies. *Hist Liq Rocket Engine Dev United States, 1955-1980*. 2014;6(224):69-122. doi:10.1126/scitranslmed.3007094.Detection

79. Agarwal B, Abu-Hamda E, Molke KL, Correa AM, Ho L. Endoscopic ultrasound-guided fine needle aspiration and multidetector spiral CT in the diagnosis of pancreatic cacer. *Am J Gastroenterol*. 2004;99(5):844-850. doi:10.1111/j.1572-0241.2004.04177.x

80. Hadano N, Murakami Y, Uemura K, et al. Prognostic value of circulating tumour DNA in

patients undergoing curative resection for pancreatic cancer. *Br J Cancer*. 2016;115(1):59-65. doi:10.1038/bjc.2016.175

81. Nakano Y, Kitago M, Matsuda S, et al. KRAS mutations in cell-free DNA from preoperative and postoperative sera as a pancreatic cancer marker: A retrospective study. *Br J Cancer*. 2018;118(5):662-669. doi:10.1038/bjc.2017.479

82. Lee B, Lipton L, Cohen J, et al. Circulating tumor DNA as a potential marker of adjuvant chemotherapy benefit following surgery for localized pancreatic cancer. *Ann Oncol*. 2019;30(9):1472-1478. doi:10.1093/annonc/mdz200

83. Groot VP, Mosier S, Javed AA, et al. Circulating tumor DNA as a clinical test in resected pancreatic cancer. *Clin Cancer Res*. 2019;25(16):4973-4984. doi:10.1158/1078-0432.CCR-19-0197

84. Eissa MAL, Lerner L, Abdelfatah E, et al. Promoter methylation of ADAMTS1 and BNC1 as potential biomarkers for early detection of pancreatic cancer in blood. *Clin Epigenetics*. 2019;11(1):1-10. doi:10.1186/s13148-019-0650-0

85. Bernard V, Kim DU, San Lucas FA, et al. Circulating Nucleic Acids Are Associated With Outcomes of Patients With Pancreatic Cancer. *Gastroenterology*. 2019;156(1):108-118.e4. doi:10.1053/j.gastro.2018.09.022

86. Cheng H, Liu C, Jiang J, et al. Analysis of ctDNA to predict prognosis and monitor treatment responses in metastatic pancreatic cancer patients. *Int J Cancer*. 2017;140(10):2344-2350. doi:10.1002/ijc.30650

87. Lee JS, Rhee TM, Pietrasz D, et al. Circulating tumor DNA as a prognostic indicator in resectable pancreatic ductal adenocarcinoma: A systematic review and meta-analysis. *Sci Rep*. 2019;9(1):1-7. doi:10.1038/s41598-019-53271-6

88. Watanabe F, Suzuki K, Tamaki S, et al. Longitudinal monitoring of KRAS-mutated circulating tumor DNA enables the prediction of prognosis and therapeutic responses in patients with pancreatic cancer. *PLoS One*. 2019;14(12):1-17. doi:10.1371/journal.pone.0227366

89. Henriksen SD, Madsen PH, Larsen AC, et al. Cell-free DNA promoter hypermethylation in plasma as a predictive marker for survival of patients with pancreatic adenocarcinoma. *Oncotarget*. 2017;8(55):93942-93956. doi:10.18632/oncotarget.21397

90. Henriksen SD, Madsen PH, Larsen AC, et al. Promoter hypermethylation in plasma-derived cell-free DNA as a prognostic marker for pancreatic adenocarcinoma staging. *Int J cancer*. 2017;141(12):2489-2497. doi:10.1002/ijc.31024

91. Pietrasz D, Wang-Renault S, Dahan L, et al. Methylated circulating tumor DNA (Met-DNA) as an independent prognostic factor in metastatic pancreatic adenocarcinoma (mPAC) patients. *J Clin Oncol*. 2019;37(15_suppl):4136. doi:10.1200/JCO.2019.37.15_suppl.4136

92. Singh N, Gupta S, Pandey RM, Chauhan SS, Saraya A. High levels of cell-free circulating nucleic acids in pancreatic cancer are associated with vascular encasement, metastasis and poor survival. *Cancer Invest*. 2015;33(3):78-85. doi:10.3109/07357907.2014.1001894

93. Vietsch EE, Graham GT, McCutcheon JN, et al. Circulating cell-free DNA mutation patterns in early and late stage colon and pancreatic cancer. *Cancer Genet*. 2017;218-219:39-50. doi:10.1016/j.cancergen.2017.08.006

94. Hu ZI, Shia J, Stadler ZK, et al. Evaluating mismatch repair deficiency in pancreatic adenocarcinoma: Challenges and recommendations. *Clin Cancer Res*. 2018;24(6):1326-1336. doi:10.1158/1078-0432.CCR-17-3099

95. Marabelle A, Le DT, Ascierto PA, et al. Efficacy of pembrolizumab in patients with noncolorectal high microsatellite instability/ mismatch repair–deficient cancer: Results from the phase II KEYNOTE-158 study. *J Clin Oncol*. 2020;38(1):1-10. doi:10.1200/JCO.19.02105

96. Golan T, Hammel P, Reni M, et al. Maintenance Olaparib for Germline BRCA -Mutated Metastatic Pancreatic Cancer . *N Engl J Med*. 2019;381(4):317-327. doi:10.1056/nejmoa1903387

97. Jones MR, Williamson LM, Topham JT, et al. NRG1 gene fusions are recurrent, clinically actionable gene rearrangements in KRAS wild-type pancreatic ductal adenocarcinoma. *Clin Cancer Res*. 2019;25(15):4674-4681. doi:10.1158/1078-0432.CCR-19-0191

98. Dahan L, Phelip JM, Le Malicot K, et al. FOLFIRINOX until progression, FOLFIRINOX with maintenance treatment, or sequential treatment with gemcitabine and FOLFIRI.3 for first-line treatment of metastatic pancreatic cancer: A randomized phase II trial (PRODIGE 35-PANOPTIMOX). *J Clin Oncol*. 2018;36(15_suppl):4000.

doi:10.1200/JCO.2018.36.15_suppl.4000

99. Rinaldi Y, Pointet AL, Khemissa Akouz F, et al. Gemcitabine plus nab-paclitaxel until progression or alternating with FOLFIRI.3, as first-line treatment for patients with metastatic pancreatic adenocarcinoma: The Federation Francophone de Cancérologie Digestive-PRODIGE 37 randomised phase II study (FIR. *Eur J Cancer*. 2020;136:25-34. doi:10.1016/j.ejca.2020.05.018

100. Bachet JB, Hammel P, Desramé J, et al. Nab-paclitaxel plus either gemcitabine or simplified leucovorin and fluorouracil as first-line therapy for metastatic pancreatic adenocarcinoma (AFUGEM GERCOR): a non-comparative, multicentre, open-label, randomised phase 2 trial. *Lancet Gastroenterol Hepatol*. 2017;2(5):337-346. doi:10.1016/S2468-1253(17)30046-8

101. Lister R, O'Malley RC, Tonti-Filippini J, et al. Highly Integrated Single-Base Resolution Maps of the Epigenome in Arabidopsis. *Cell*. 2008;133(3):523-536. doi:10.1016/j.cell.2008.03.029

102. Emrich SJ, Barbazuk WB, Li L, Schnable PS. Gene discovery and annotation using LCM-454 transcriptome sequencing. *Genome Res*. 2007;17(1):69-73. doi:10.1101/gr.5145806

103. Dobin A, Davis CA, Schlesinger F, et al. STAR: Ultrafast universal RNA-seq aligner. *Bioinformatics*. 2013;29(1):15-21. doi:10.1093/bioinformatics/bts635

104. Liao Y, Smyth GK, Shi W. FeatureCounts: An efficient general purpose program for assigning sequence reads to genomic features. *Bioinformatics*. 2014;30(7):923-930. doi:10.1093/bioinformatics/btt656

105. Hilmi M, Cros J, Puleo F, et al. Tumour and stroma RNA signatures predict more accurately distant recurrence than clinicopathological factors in resected pancreatic adenocarcinoma. *Eur J Cancer*. 2021;148:171-180. doi:10.1016/j.ejca.2021.01.042

106. Bankhead P, Loughrey MB, Fernández JA, et al. QuPath: Open source software for digital pathology image analysis. *Sci Rep*. 2017;7(1):1-7. doi:10.1038/s41598-017-17204-5

Appendix

Résumé substantiel français

Introduction

L'adénocarcinome pancréatique (AP) est l'un des cancers digestifs les plus fréquents. Selon le GLOBOCAN 2020[1], il représente 2,6% des cancers dans le monde. En 2020, un AP a été diagnostiqué chez 495773 patients[1]. Le nombre de cas chez les hommes (262865 cas) est un peu plus élevé que chez les femmes (232908 cas) [1]. Les personnes âgées sont plus susceptibles de développer cette maladie avec, sur l'ensemble des patients diagnostiqués en 2020, 396844 (80%) patients de plus de soixante ans. Les pays développés (en particulier les pays européens et les États-Unis) ont montré une incidence plus élevée que les autres pays[1]. L'incidence des APs devrait presque doubler en 20 ans. L'augmentation du taux est plus rapide dans les pays en développement et les pays sous-développés (Asie, Amérique latine et Caraïbes, et Afrique).
L'AP est une tumeur solide maligne de mauvais pronostic. Malgré son incidence relativement faible, ce cancer représente 4,7 % de la mortalité liée au cancer. La survie globale à 5 ans n'est que de 9 %, soit la plus faible de tous les cancers[2]. La détection précoce des APs reste un défi pour la pratique clinique. Au moment du diagnostic, seulement 15 à 20 % des patients peuvent bénéficier d'une résection à visée curative[3]. La chimiothérapie systémique est le traitement standard des APs localement avancées et métastatiques.
La gemcitabine en monothérapie a été le traitement standard des APs avancées pendant plus de dix ans[4]. En 2011, le résultat d'un essai clinique de phase III a montré que le régime FOLFIRINOX (association d'oxaliplatine, d'irinotécan, de fluorouracile et de leucovorine) était associé à un avantage de survie mais à un profil de toxicité accru chez les patients atteints de APs métastatique[5]. Pour les patients ayant une AP réséquée, l'utilisation du régime FOLFIRINOX modifié comme traitement adjuvant a également montré une survie significativement plus longue que la monothérapie par gemcitabine au détriment d'une incidence plus élevée d'effets secondaires[6]. Le FOLFIRINOX est une option pour traiter les patients ayant un bon indice de performance et un taux de bilirubinémie normal. Un autre essai clinique de phase III a montré que l'association nab-paclitaxel et gemcitabine améliorait significativement la survie globale, la survie sans progression et le taux de réponse chez les patients atteints d'AP métastatique, mais les taux de neuropathie périphérique et de myélosuppression étaient augmentés[7].
Par rapport aux progrès de la chimiothérapie, l'intérêt de la radiochimiothérapie pour le traitement des APs localement avancés ou de résécabilité limite est encore en discussion. Les essais cliniques n'ont pas permis de démontrer que la radiochimiothérapie était associée à une augmentation de la survie globale en adjuvant et en situation localement avancée[8,9].
Pour améliorer le taux de résection R0 et le pronostic des APs résécables, de résécabilité limite ou localement avancées, des stratégies thérapeutiques néoadjuvantes/induction associant chimiothérapie avec ou sans radiochimiothérapie sont en cours de développement[10]. Le premier essai clinique de thérapie néoadjuvante pour les APs a été rapporté en 2015 mais aucune différence significative n'était retrouvée entre les deux bras[11]. L'étude ESPAC-5F a recruté 90

patients résécables borderline et les a divisés en quatre bras (chirurgie d'emblée, GEMCAP, FOLFIRINOX et radiochimiothérapie). Les résultats ont montré qu'il n'y avait pas de différence de taux de résection entre les bras. Cependant, le traitement d'induction (tous bras confondus) était associé à un bénéfice significatif en termes de survie par rapport à la chirurgie d'emblée[12].
Chez les patients avec un AP de résécabilité limite ou localement avancé, plusieurs centres ont rapporté un taux élevé de résection secondaire après traitement d'induction, pouvant aller jusqu'à 60 %[13,14,15]. Le FOLFIRINOX est le principal protocole ayant été utilisé dans ces études et est considéré comme un des régimes thérapeutiques le plus prometteur.
Malgré quelques progrès récents, les APs restent radio- et chimiorésistantes et le pronostic global des patients à tous les stades s'est peu amélioré. Pour décrire l'hétérogénéité des APs et le bénéfice de la chimiothérapie, plusieurs équipes ont utilisé des techniques de biologie moléculaire pour mieux caractériser les APs. Collinson et al[16] ont rapporté le premier profilage transcriptomique d'AP au monde. Pour prédire le bénéfice du traitement adjuvant avec gemcitabine, Nicolle et al[17] ont décrit une signature transcriptomique de sensibilité à la Gemcitabine. Ces études translationnelles ont montré la nécessité de mieux caractériser les APs en utilisant les méthodes de biologie moléculaire et de développer des biomarqueurs robustes pour guider la pratique clinique.
Comparés aux biomarqueurs tissulaires, qui nécessitent une procédure invasive, les biomarqueurs plasmatiques ou « biopsie liquide » peuvent également aider au diagnostic, au pronostic et à l'évaluation de la chimio sensibilité dans la médecine de précision personnalisée. Les principaux biomarqueurs de biopsie liquide comprennent les cellules tumorales circulantes (CTC), l'ADN tumoral circulant (ADNtc), les vésicules extracellulaires (VEs) et les exosomes[18–22].
La détection de l'ADNtc semble être un outil utilisable pour la prise en charge des patients atteints d'AP. La valeur pronostique de l'ADNtc a été observée dans plusieurs études[23,24,25]. Pour prédire de manière précoce l'efficacité de la chimiothérapie, pour évaluer la maladie résiduelle minimale après la chirurgie et la récidive après résection à visée curative, l'ADNtc a été considéré comme un biomarqueur potentiellement utile[26,27,28]. Le taux de détection de l'ADNtc augmente du stade I au stade IV[23], mais il n'est toujours pas détectable chez un certain nombre de patients, même à un stade avancé[29]. La raison de ce phénomène n'est pas claire.

Patients et Méthodes

Patients

Les cohortes de patients suivantes ont été utilisées dans l'étude.

Cohorte RASPANC

De mai 2011 à mai 2018, les plasmas de tous les patients consécutifs atteints d'AP histologiquement prouvé recevant une chimiothérapie systémique ont été collectés prospectivement à l'hôpital de la Pitié Salpêtrière (Paris, France), y compris les stades résécables et métastatiques. Des échantillons de sang ont été prélevés juste avant (i) le premier cycle de traitement adjuvant, après résection chirurgicale chez les patients ayant eu une résection à visée curative (R0/R1), ou (ii) le premier jour du cycle de chimiothérapie chez les patients présentant une maladie métastatique. Les échantillons de sang ont été centrifugés à 3 500 tr/min pendant 15 minutes à 4°C dans les 3 heures suivant la prise de sang. Le plasma a été stocké à -80°C jusqu'à une utilisation future. Cette étude a été menée conformément aux principes de la Conférence Internationale d'Harmonisation des Bonnes Pratiques Cliniques et de la Déclaration d'Helsinki et a été approuvée par un comité d'éthique indépendant (CPP Ile-de-France 2014/58NICB et 2014/59NICB). Tous les patients ont signé un formulaire de consentement éclairé. Pour les patients métastatiques, les patients sans bloc FFPE disponible ou qui n'avaient eu qu'une aspiration à l'aiguille fine sous endoscopie échographique ont été exclus. Un pathologiste spécialisé en pathologie pancréatique (J.A.) a confirmé le diagnostic d'adénocarcinome, a sélectionné des carottes représentatives (1 carotte de 1,5 mm de diamètre pour l'extraction d'ARN et 4 carottes de 1 mm de diamètre pour le TMA) après examen de la lame colorée H&E. Les données suivantes ont été recueillies dans une base de données prospective : caractéristiques cliniques et pathologiques (sexe, âge, antécédents médicaux, date du diagnostic, localisation de la tumeur primitive, diamètre de la tumeur primitive, grade de différenciation tumorale et stade de la maladie), données de suivi (date de résection primaire, date et type de rechute, date de diagnostic de la maladie métastatique, date et protocole de chimiothérapie, date et protocole de radiochimiothérapie, date de décès ou du dernier suivi). Le stade TNM a été redéfini selon la 8e édition de l'AJCC par les données initialement collectées. La marge de résection R1 était définie comme une distance de la tumeur à la marge de résection < ou = 1 mm.

Cohorte Beaujon

D'avril 1997 à avril 2009, les patients avec AP résécable opérés à l'hôpital Beaujon (Paris, France) ont été rétrospectivement inclus. Les critères d'exclusion étaient la chimiothérapie ou la radiothérapie préopératoire, la résection incomplète macroscopique (R2), l'adénocarcinome de l'ampoule Vater ou les tumeurs pancréatiques autres que l'adénocarcinome. Les patients décédés de complications postopératoires au cours des 30 jours suivant la chirurgie ont également été exclus car ils n'étaient pas informatifs pour l'étude translationnelle. Cette étude a été menée conformément aux principes de la Conférence Internationale d'Harmonisation des Bonnes Pratiques Cliniques et de la Déclaration d'Helsinki et a été approuvée par un comité d'éthique indépendant (CPP Ile-de-France 2014/58NICB et 2014/59NICB). Les échantillons tumoraux inclus dans cette étude provenaient de soins de routine, et aucun échantillon supplémentaire n'a été prélevé dans le cadre de cette étude. Une note d'information a été remise au patient pour l'informer de l'utilisation de ses échantillons pour de futures analyses moléculaires. Les patients avaient la possibilité de signer une note d'opposition à une telle analyse. Tous les patients inclus ont accepté de participer. Un pathologiste pancréatique spécialisé (J.C.) a confirmé la présence de cellules néoplasiques, a sélectionné un bloc tumoral FFPE représentatif après examen des

lames colorées par H&E et a donné une estimation visuelle de la cellularité tumorale. Deux carottes de 1,5 mm de diamètre dans la zone tumorale ont été extraites pour l'extraction d'ARN.

Cohorte multicentrique française

Cette cohorte multicentrique (Hôpitaux Pitié Salpêtrière, Saint Antoine et Ambroise Paré) a inclus 165 patients parmi les 309 patients inclus dans notre étude précédente[62]. Pour ces 165 patients, suffisamment d'ARN restant était disponible. Pour chaque cas, des coupes entières de lame ont été examinées pour sélectionner des zones enrichies en tumeurs. Deux carottes d'un diamètre de 1,5 mm ont été extraites du bloc de paraffine dans cette zone pour l'extraction d'ARN/ADN.

PRODIGE 35 Cohorte

PRODIGE 35 est un essai de phase II prospectif, ouvert, multicentrique, randomisé, évaluant une chimiothérapie de maintenance (FOLFIRINOX +/- LV5FU2) dans le traitement de première intention des APs métastatiques. Les patients étaient randomisés entre trois bras dans cette étude (NCT02352337) : Bras A, FOLFIRINOX toutes les deux semaines jusqu'à progression de la maladie ou apparition d'une réaction de toxicité intolérable (12 cycles maximum) ; Bras B, après huit cycles de FOLFIRINOX, en cas de contrôle de la maladie, maintenance par LV5FU2 jusqu'à progression de la maladie (reprise de FOLFIRINOX à progression) ; Bras C, administration séquentielle de FOLFIRI3 et de gemcitabine, alternativement toutes les 8 semaines, jusqu'à progression ou toxicité inacceptable. Des échantillons de sang ont été prélevés à l'inclusion et envoyés dans les 24 heures au laboratoire central. Les échantillons ont été centrifugés à 3500 tr/min pendant 15 minutes à 4°C. Le plasma a été stocké à -80°C jusqu'à une utilisation future. A partir des prélèvements tumoraux diagnostiques, un pathologiste pancréatique spécialisé (J.C.) a confirmé la présence de cellules néoplasiques, a sélectionné un bloc tumoral FFPE représentatif après examen des lames colorées par H&E et a donné une estimation visuelle de la cellularité tumorale. Pour les échantillons de tissus, six lames de 10 mm ont été découpées et microdisséquées manuellement pour enrichir en cellules néoplasiques. Pour les échantillons d'aspiration cellulaire, six lames de 10 mm ont été découpées et toutes les lames ont été utilisées pour l'extraction d'ARN/ADN.

PRODIGE 37 Cohorte

PRODIGE 37 est un essai de phase II prospectif, multicentrique, randomisé évaluant le traitement séquentiel par nab-paclitaxel + gemcitabine et FOLFIRI3 (en alternance) versus Nab-Paclitaxel + Gemcitabine dans le traitement de première ligne des APs métastatiques (NCT02827201). Les patients étaient randomisés entre deux bras dans cette étude : Bras A, administration séquentielle de nab-paclitaxel + gemcitabine et FOLFIRI3, alternativement toutes les 8 semaines, jusqu'à progression ou toxicité inacceptable ; Bras B, nab-paclitaxel + gemcitabine jusqu'à progression ou toxicité inacceptable. Des échantillons de sang ont été prélevés à l'inclusion et envoyés dans les 24 heures au laboratoire central. Les échantillons ont été centrifugés à 3500 tr/min pendant 15 minutes à 4°C. Le plasma a été stocké à -80°C jusqu'à une utilisation future. A partir des prélèvements tumoraux diagnostiques, un pathologiste pancréatique spécialisé (J.C.) a confirmé la présence de cellules néoplasiques, a sélectionné un bloc tumoral FFPE représentatif après examen des lames colorées par H&E et a donné une estimation visuelle de la cellularité tumorale. Pour les échantillons de tissus, six lames de 10 mm ont été découpées et microdisséquées manuellement pour enrichir en cellules néoplasiques. Pour les échantillons d'aspiration cellulaire, six lames de 10 mm ont été découpées et toutes les lames ont été utilisées pour l'extraction d'ARN/ADN.

Cohorte AFUGEM

AFUGEM est un essai de phase II non comparatif, multicentrique, ouvert et randomisé évaluant le nab-paclitaxel plus soit la gemcitabine soit le LV5FU2 dans le traitement de première intention des APs métastatiques (NCT01964534). Les patients étaient randomisés entre deux bras dans cette étude : Bras A, nab-paclitaxel + gemcitabine jusqu'à progression ou toxicité inacceptable ; Bras B, nab-paclitaxel + LV5FU2 jusqu'à progression ou toxicité inacceptable. A partir des prélèvements tumoraux diagnostiques, un pathologiste pancréatique spécialisé (J.C.) a confirmé la présence de cellules néoplasiques et a sélectionné un bloc tumoral FFPE représentatif après examen des lames colorées par H&E. Pour les échantillons de tissus, six lames de 10 mm ont été découpées et microdisséquées manuellement pour enrichir en cellules néoplasiques. Pour les échantillons d'aspiration cellulaire, six lames de 10 mm ont été découpées et toutes les lames ont été utilisées pour l'extraction d'ARN.

L'extraction d'ARN et séquençage de l'ARN

Pour la cohorte RASPANC, la cohorte BEAUJON et la cohorte AFUGEM, nous n'avons extrait que les ARN. Le kit RNeasy FFPE (Qiagen©, Allemagne) a été utilisé dans la cohorte RASPANC et la cohorte BEAUJON. Le kit miRNeasy FFPE (Qiagen©, Allemagne) a été utilisé dans la cohorte AFUGEM. Pour la cohorte française multicentrique, les cohortes PRODIGE 35 et PRODIGE 37, nous avons extrait à la fois les ADN et les ARN. Le kit de tissus ALLPrep FFPE (Qiagen©, Venlo, Pays-Bas) a été utilisé pour la double extraction dans ces cohortes. L'extraction a été réalisée selon les recommandations du fabricant.

Nous avons utilisé le kit de préparation de bibliothèque Lexogen QuantSeq 3'mRNA-Seq FWD (Lexogen Gmbh, Autriche) pour toutes les cohortes, à l'exception de la cohorte AFUGEM. Pour la cohorte AFUGEM, la plupart des échantillons sont des échantillons cytologiques et ont donné lieu à une faible concentration de solution d'ARN. Le SMARTer Stranded Total RNA-Seq Kit v3 Pico Input Mammalian (Takara Bio, USA) a été sélectionné pour cette cohorte en raison de son avantage pour les faibles concentrations d'ARN.

Les lectures RNAseq ont été cartographiées à l'aide de STAR[30] avec les paramètres ENCODE proposés sur les génomes hg38 humains et l'annotation des transcrits (Ensembl 75). Les profils d'expression génique ont été obtenus à l'aide de FeatureCount[31].

Nous avons précédemment décrit[32] six composants d'ARN par analyse des composants indépendants (ACI))[33] basée sur le résultat d'Affymetrix[32,34]. Ces composants peuvent décrire quantitativement la composition de la tumeur (composant tumoral de type basal et composant tumoral classique) et du stroma (composant stroma activé, composant stroma structurel inactif, composant stroma inflammatoire et composant stroma immunitaire). En utilisant la référence de ces six composants, nous avons projeté les niveaux des composantes de la présente étude.

Nous avons également publié le centroïde de chacun des 5 sous-types (classique pur, classique immunitaire, desmoplastique, stroma activé et de type basal pur). Cette classification de sous-type était à l'origine regroupée par regroupement non supervisé et désignée par l'expression de ces six niveaux de composants. Le centroïde comprend la valeur moyenne d'expression de sous-type de 404 gènes sélectionnés. Le profil d'expression génique sélectionné dans la présente étude a ensuite été corrélé à chacun des 5 centroïdes à l'aide de la corrélation de rang de Spearman, comme publié précédemment ; le centroïde de sous-type avec la corrélation la plus élevée définit la classe prédite des échantillons de test dans la présente étude.

La caractérisation moléculaire aboutit à deux types de phénotypage d'échantillons. Le sous-typage a abouti à une classification dans laquelle chaque patient se trouve être membre de l'un des 5 sous-types. En revanche, la projection sur les 6 composants a abouti, pour chaque patient, à 6 scores mesurant le niveau relatif de chaque phénotype tumoral et stromal codé par les 6

composants. À des fins de représentation, les projections des composants ont ensuite été mises à l'échelle de sorte que chaque composant ait une moyenne de 0 et un écart-type de 1. En fin de compte, la classification en 5 sous-types aboutit à une variable qualitative (avec cinq modalités), tandis que les projections des composants aboutissent à 6 variables quantitatives (une pour chaque composant).

L'extraction de l'ADN Circulant du Plasma et NGS

Des échantillons de sang (9 ml) ont été prélevés à partir d'un cathéter central avant l'administration de la chimiothérapie et placés dans des tubes EDTA. Le kit QIAamp Circulating Nucleic Acid (Qiagen, Allemagne) a été utilisé pour l'extraction d'ADN. Des bibliothèques de séquençage ont été préparées à partir d'ADNtc en utilisant Ion AmpliSeq Colon et Lung Cancer Research Panel v2 (Thermo Fisher, USA). La procédure a été effectuée comme décrit précédemment[23].

Construction de TMA et interprétation

Nous avons utilisé la cohorte GHPS pour construire la puce à ADN tissulaire. Pour chaque bloc FFPE, quatre cylindres de tissu d'un diamètre de 1 mm ont été perforés à partir du centre de la tumeur. Ces cylindres ont été introduits dans un bloc de paraffine receveur à l'aide d'un dispositif manuel de tissu arrayer MTA Booster OI (Alphelys, Plaisir, France). Les anticorps primaires suivants ont été utilisés aux dilutions indiquées : anticorps primaire monoclonal de lapin anti-CD4 (SP35) (dilution 1:4 ; clone SP35 ; Ventana, USA) ; anticorps monoclonal de souris anti-CD8 humain (dilution 1:100; clone C8/144; Dako, Danemark); anticorps monoclonal de souris anti-CD68 humain (dilution 1:50; clone KP1; Dako, Danemark); anticorps monoclonal de lapin anti-FoxP3 humain (dilution 1:100; clone SP97; Spring Bioscience, USA); anticorps monoclonal t-bet (dilution 1:100; clone 4B10; eBioscience, USA); anticorps monoclonal de souris PD-1 (prédilué ; clone NAT105 ; Sigma-Aldrich, USA) ; Anticorps monoclonal de lapin PD-L1 (dilution 1:100; clone NAT105; BIOCYC, Allemagne). La procédure d'immunomarquage a été réalisée sur des coupes de TMA fixées au formol, déparaffinées, de 4 mm d'épaisseur, selon le protocole du fabricant. Des lames de verre TMA ont été numérisées pour produire des lames numériques (0,25 mm/pixel à un grossissement de 40x) à l'aide du système de numérisation de diapositives Aperio (ScanScope CS ; Aperio Technologies, États-Unis). Les cellules positives dans un millimètre carré de CD4, CD8, CD68, FoxP3 et t-bet ont été comptées à l'aide du logiciel QuPath développé par l'université d'Édimbourg[35]**.** Les carottes colorées PD-1 et PD-L1 ont été notées par deux chercheurs indépendamment des informations clinicopathologiques. Le pourcentage de cellules positives dans le parenchyme des tumeurs a été compté pour PD-1. Le pourcentage de cellules positives dans le parenchyme et le mésenchyme des tumeurs a été compté séparément pour PD-L1. La valeur médiane des 4 scores pour chaque patient a été calculée pour une étude statistique plus approfondie.

L'objet de thèse

L'objet de cette thèse est de mieux caractériser l'AP à l'aide du RNA-seq et de l'ADNtc. Nous avons publié/soumis les résultats obtenus dans la cohorte de patients ayant subi une résection à visée curative. Pour les cohortes de patients métastatiques, nous avons terminé les manipulations et les analyses statistiques sont en cours.

Résultats et Conclusion

Pour la première étude chez les patients réséqués à visée curative d'un AP. 210 patients d'une cohorte multicentrique (cohorte multicentrique française et cohorte RASPANC) et 149 patients d'une cohorte monocentrique (cohorte Beaujon) ont été inclus dans cette étude. Les profils d'ARN micro-array ont été obtenus à partir de 165 patients de la cohorte multicentrique. Les profils de séquençage de l'ARN ont été obtenus pour tous les patients. Pour les patients présentant à la fois des profils d'ARN micro-array et RNA-seq, la concordance dans l'attribution des sous-types était partielle avec un taux de cohérence de 82,4 %. La corrélation entre les deux projections techniques des six composants variait de 0,85 à 0,95, démontrant un avantage de robustesse. Sur la base du critère d'information d'Akaike, les composants d'ARN ont montré plus de valeur pronostique dans les modèles univariés ou multivariés que les sous-types. En utilisant la cohorte monocentrique comme cohorte test, nous avons développé un modèle de régression de Cox multivarié utilisant les six composants et les caractéristiques clinicopathologiques (invasion ganglionnaire et marges de résection) sur SSM. Ce modèle pronostique était fortement associé à la SSM ($p<0,001$). La validation du modèle dans la cohorte multicentrique a montré une association significative avec la SSM et la SG ($p<0,001$). Nous avons décrit l'avantage de la valeur pronostique et de la robustesse des composants transcriptomiques de la tumeur entière par rapport aux sous-types. Nous avons créé et validé un nouveau modèle pronostique de régression de Cox multivarié basé sur SSM, comprenant six niveaux de composants transcriptomiques de AP et des caractéristiques pathologiques.
Pour la seconde partie des patients réséqués, la cohorte RASPANC a été utilisée. Parmi les 47 patients éligibles, 2 patients sans échantillon de tissu suffisant ont été exclus, 45 patients ont été inclus pour l'étude. Avant le début de la chimiothérapie adjuvante, l'ADNtc était détectable chez 6 (13 %) patients. Les tumeurs associées à un ADNtc détectable ont montré des scores de composant tumoral de type basal ($p = 0,037$) et de composant de stroma activé ($p = 0,002$) plus élevés. Ces tumeurs ont été observées avec moins de lymphocytes CD8 positifs infiltrés en immunohistochimie (TMA) ($p=0,008$) et via l'algorithme de prédiction du profil transcriptomique ($p<0,001$). Les lymphocytes CD8 positifs (coefficient=-0,320, $p=0,032$) et les lymphocytes positifs PD-1 (coefficient=-0,356, $p=0,016$) étaient négativement corrélés avec le composant tumoral de type basal.
Nos résultats suggèrent que les patients dont les tumeurs sont constituées de composants tumoraux dominants de type basal sont plus susceptibles de présenter un ADNtc et présenteraient un statut de « désert immunitaire » tumoral. Cependant, les interactions derrière ce phénomène ne sont pas claires et doivent être étudiées dans d'autres études.
Pour les patients métastatiques, toutes les manipulations sont terminées et l'analyse des données se poursuit. Nous allons étudier les profils transcriptomiques des APs métastatiques (composants et sous-types), la valeur pronostique et la valeur prédictive de la classification des sous-types et des différents composants pour l'efficacité des protocoles de chimiothérapie utilisés ainsi que leur corrélation avec la présence d'ADNtc.
Nos études devraient aider à mieux comprendre les sous-types des APs primaires et métastatiques définis selon le transcriptome. La précision et les modèles complets développés dans nos études pourraient être utiles pour développer des protocoles de médecine personnalisée chez les patients avec un AP.

Référence

1. Sung H, Ferlay J, Siegel RL, et al. Global Cancer Statistics 2020: GLOBOCAN Estimates of Incidence and Mortality Worldwide for 36 Cancers in 185 Countries. *CA Cancer J Clin*. 2021;71(3):209-249. doi:10.3322/caac.21660

2. Siegel RL, Miller KD, Jemal A. Cancer statistics, 2020. *CA Cancer J Clin*. 2020;70(1):7-30. doi:10.3322/caac.21590

3. Li D, Xie K, Wolff R, Abbruzzese JL. Pancreatic cancer. *Lancet (London, England)*. 2004;363(9414):1049-1057. doi:10.1016/S0140-6736(04)15841-8

4. Howard B, Iii AB, Moore MJ, et al. Improvements in Survival and Clinical Benefit With Gemcitabine as First-Line Therapy for Patients With Advanced Pancreas Cancer : A Randomized Trial. *J Clin Oncol*. 1997;15(6):2403-2413.

5. Conroy T, Desseigne F, Ychou M, et al. FOLFIRINOX versus Gemcitabine for Metastatic Pancreatic Cancer. *N Engl J Med*. 2011;364(19):1817-1825. doi:10.1056/nejmoa1011923

6. Conroy T, Hammel P, Hebbar M, et al. FOLFIRINOX or Gemcitabine as Adjuvant Therapy for Pancreatic Cancer. *N Engl J Med*. 2018;379(25):2395-2406. doi:10.1056/nejmoa1809775

7. Von Hoff DD, Ervin T, Arena FP, et al. Increased Survival in Pancreatic Cancer with nab-Paclitaxel plus Gemcitabine. *N Engl J Med*. 2013;369(18):1691-1703. doi:10.1056/nejmoa1304369

8. Neoptolemos JP, Stocken DD, Friess H, et al. A Randomized Trial of Chemoradiotherapy and Chemotherapy after Resection of Pancreatic Cancer. *N Engl J Med*. 2004;350(12):1200-1210. doi:10.1056/nejmoa032295

9. Hammel P, Huguet F, Van Laethem J-L, et al. Comparison of chemoradiotherapy (CRT) and chemotherapy (CT) in patients with a locally advanced pancreatic cancer (LAPC) controlled after 4 months of gemcitabine with or without erlotinib: Final results of the international phase III LAP 07 study. *J Clin Oncol*. 2013;31(18_suppl):LBA4003-LBA4003. doi:10.1200/jco.2013.31.18_suppl.lba4003

10. Bockhorn M, Uzunoglu FG, Adham M, et al. Borderline resectable pancreatic cancer: A consensus statement by the International Study Group of Pancreatic Surgery (ISGPS). *Surg (United States)*. 2014;155(6):977-988. doi:10.1016/j.surg.2014.02.001

11. Golcher H, Brunner TB, Witzigmann H, et al. Neoadjuvant chemoradiation therapy with gemcitabine/cisplatin and surgery versus immediate surgery in resectable pancreatic cancer: Results of the first prospective randomized phase II trial. *Strahlentherapie und Onkol*. 2015;191(1):7-16. doi:10.1007/s00066-014-0737-7

12. Ghaneh P, Palmer DH, Cicconi S, et al. ESPAC-5F: Four-arm, prospective, multicenter, international randomized phase II trial of immediate surgery compared with neoadjuvant gemcitabine plus capecitabine (GEMCAP) or FOLFIRINOX or chemoradiotherapy (CRT) in patients with borderline resectable pan. *J Clin Oncol*. 2020;38(15_suppl):4505. doi:10.1200/JCO.2020.38.15_suppl.4505

13. Ferrone CR, Marchegiani G, Hong TS, et al. Radiological and surgical implications of

neoadjuvant treatment with FOLFIRINOX for locally advanced and borderline resectable pancreatic cancer. *Ann Surg*. 2015;261(1):12-17. doi:10.1097/SLA.0000000000000867

14. Nitsche U, Wenzel P, Siveke JT, et al. Resectability After First-Line FOLFIRINOX in Initially Unresectable Locally Advanced Pancreatic Cancer: A Single-Center Experience. *Ann Surg Oncol*. 2015;22:1212-1220. doi:10.1245/s10434-015-4851-2

15. Petrelli F, Coinu A, Borgonovo K, et al. FOLFIRINOX-based neoadjuvant therapy in borderline resectable or unresectable pancreatic cancer: A meta-analytical review of published studies. *Pancreas*. 2015;44(4):515-521. doi:10.1097/MPA.0000000000000314

16. Collisson EA, Sadanandam A, Olson P, et al. Subtypes of pancreatic ductal adenocarcinoma and their differing responses to therapy. *Nat Med*. 2011;17(4):500-503. doi:10.1038/nm.2344

17. Nicolle R, Gayet O, Duconseil P, et al. A transcriptomic signature to predict adjuvant gemcitabine sensitivity in pancreatic adenocarcinoma. *Ann Oncol*. 2020;xxx(xxx). doi:10.1016/j.annonc.2020.10.601

18. Vaidyanathan R, Soon RH, Zhang P, Jiang K, Lim CT. Cancer diagnosis: from tumor to liquid biopsy and beyond. *Lab Chip*. 2019;19(1):11-34. doi:10.1039/c8lc00684a

19. Ignatiadis M, Sledge GW, Jeffrey SS. Liquid biopsy enters the clinic - implementation issues and future challenges. *Nat Rev Clin Oncol*. 2021;18(5):297-312. doi:10.1038/s41571-020-00457-x

20. Von Felden J, Garcia-Lezana T, Schulze K, Losic B, Villanueva A. Liquid biopsy in the clinical management of hepatocellular carcinoma. *Gut*. 2020;69(11):2025-2034. doi:10.1136/gutjnl-2019-320282

21. Hofman P, Heeke S, Alix-Panabières C, Pantel K. Liquid biopsy in the era of immuno-oncology: Is it ready for prime-time use for cancer patients? *Ann Oncol*. 2019;30(9):1448-1459. doi:10.1093/annonc/mdz196

22. Normanno N, Cervantes A, Ciardiello F, De Luca A, Pinto C. The liquid biopsy in the management of colorectal cancer patients: Current applications and future scenarios. *Cancer Treat Rev*. 2018;70:1-8. doi:10.1016/j.ctrv.2018.07.007

23. Pietrasz D, Pécuchet N, Garlan F, et al. Plasma circulating tumor DNA in pancreatic cancer patients is a prognostic marker. *Clin Cancer Res*. 2017;23(1):116-123. doi:10.1158/1078-0432.CCR-16-0806

24. Kaczor-Urbanowicz KE, Cheng J, King JC, et al. Reviews on Current Liquid Biopsy for Detection and Management of Pancreatic Cancers. *Pancreas*. 2020;49(9):1141-1152. doi:10.1097/MPA.0000000000001662

25. Abdallah R, Taly V, Zhao S, et al. Plasma circulating tumor DNA in pancreatic adenocarcinoma for screening, diagnosis, prognosis, treatment and follow-up: A systematic review. *Cancer Treat Rev*. 2020;87:102028. doi:10.1016/j.ctrv.2020.102028

26. Bachet JB, Blons H, Hammel P, et al. Circulating Tumor DNA is Prognostic and Potentially Predictive of Eryaspase Efficacy in Second-line in Patients with Advanced

Pancreatic Adenocarcinoma. *Clin Cancer Res*. 2020;26(19):5208-5216. doi:10.1158/1078-0432.CCR-20-0950

27. Jiang J, Ye S, Xu Y, et al. Circulating Tumor DNA as a Potential Marker to Detect Minimal Residual Disease and Predict Recurrence in Pancreatic Cancer. *Front Oncol*. 2020;10(July):1-8. doi:10.3389/fonc.2020.01220

28. Yin L, Pu N, Thompson ED, Miao Y, Wolfgang CL, Yu J. Improved assessment of response status in patients with pancreatic cancer treated with neoadjuvant therapy using somatic mutations and liquid biopsy analysis. *Clin Cancer Res*. Published online 2020:clincanres.1746.2020. doi:10.1158/1078-0432.ccr-20-1746

29. Manuscript A, Malignancies H. Detection of Circulating Tumor DNA in Early- and Late-Stage Human Malignancies. *Hist Liq Rocket Engine Dev United States, 1955-1980*. 2014;6(224):69-122. doi:10.1126/scitranslmed.3007094.Detection

30. Dobin A, Davis CA, Schlesinger F, et al. STAR: Ultrafast universal RNA-seq aligner. *Bioinformatics*. 2013;29(1):15-21. doi:10.1093/bioinformatics/bts635

31. Liao Y, Smyth GK, Shi W. FeatureCounts: An efficient general purpose program for assigning sequence reads to genomic features. *Bioinformatics*. 2014;30(7):923-930. doi:10.1093/bioinformatics/btt656

32. Puleo F, Nicolle R, Blum Y, et al. Stratification of Pancreatic Ductal Adenocarcinomas Based on Tumor and Microenvironment Features. *Gastroenterology*. 2018;155(6):1999-2013.e3. doi:10.1053/j.gastro.2018.08.033

33. Cardoso JF, Souloumiac A. Blind beamforming for non-Gaussian signals. *IEE Proceedings, Part F Radar Signal Process*. 1993;140(6):362-370. doi:10.1049/ip-f-2.1993.0054

34. Hilmi M, Cros J, Puleo F, et al. Tumour and stroma RNA signatures predict more accurately distant recurrence than clinicopathological factors in resected pancreatic adenocarcinoma. *Eur J Cancer*. 2021;148:171-180. doi:10.1016/j.ejca.2021.01.042

35. Bankhead P, Loughrey MB, Fernández JA, et al. QuPath: Open source software for digital pathology image analysis. *Sci Rep*. 2017;7(1):1-7. doi:10.1038/s41598-017-17204-5